PERGAMON Progress in Quantum Electronics 26 (2002) 131–191

Progress in Quantum Electronics

www.elsevier.com/locate/pquantelec

Review

Optical phase conjugation: principles, techniques, and applications

Guang S. He*

Institute for Lasers, Photonics and Biophotonics, State University of New York at Buffalo, Buffalo, NY 14260-3000, USA

Abstract

Over the last three decades, optical phase conjugation (OPC) has been one of the major research subjects in the field of nonlinear optics and quantum electronics. OPC defines usually a special relationship between two coherent optical beams propagating in opposite directions with reversed wave front and identical transverse amplitude distributions. The unique feature of a pair of phase-conjugate beams is that the aberration influence imposed on the forward beam passed through an inhomogeneous or disturbing medium can be automatically removed for the backward beam passed through the same disturbing medium.

To date there have been three major technical approaches that can efficiently produce the backward phase-conjugate beam. The first approach is based on the degenerate (or partially degenerate) four-wave mixing processes, the second is based on various backward simulated (Brillouin, Raman, Rayleigh-wing or Kerr) scattering processes, and the third is based on one-photon or multi-photon pumped backward stimulated emission (lasing) processes. Among these three different approaches, there is a common physical mechanism that plays the same essential role in generating a backward phase-conjugate beam, which is the formation of the induced holographic grating and the subsequent wave-front restoration via a backward reading beam. In most experimental studies, certain types of resonance enhancements of induced refractive-index changes are desirable for obtaining higher grating-diffraction efficiency.

The momentum of OPC studies has recently become even stronger because there are more prospective potentials and achievements for applications. OPC-associated techniques can be successfully utilized in many different application areas: such as high-brightness laser oscillator/amplifier systems, cavity-less lasing devices, laser target-aiming systems, aberration correction for coherent-light transmission and reflection through disturbing media, long distance optical fiber communications with ultra-high bit-rate, optical phase locking and coupling systems, and novel optical data storage and processing systems. Published by Elsevier Science Ltd.

*Fax: +1-716-645-6945.

E-mail address: gshe@acsu.buffalo.edu (G.S. He).

0079-6727/02/$ - see front matter Published by Elsevier Science Ltd.
PII: S0079-6727(02)00004-6

PACS: 42.65.Hw

Keywords: Optical phase conjugation; Nonlinear wave-mixing; Stimulated scattering; Stimulated emission; Laser-induced phase grating; Laser holography

Contents

1. Introduction to optical phase conjugation (OPC)

Optical phase conjugation (OPC)[1] is a new laser-based technique developed since 1970s. As this technique is feasible for use in many significant applications, the study of OPC has become one of the most active research subjects in the areas of nonlinear optics and quantum electronics [1–8].

Before the 1960s and the advent of lasers, it was well known that there were two impossibilities within the regime of conventional optics. The first was that the brightness of any given light beam cannot be increased via any type of optical imaging systems or specially designed devices. The second was that a perfect and reversible optical imaging system was impossible because of the aberration influence from optical elements and propagating media. The first impossibility was removed after the advent of laser oscillators and amplifiers. The second restraint could also be released by utilizing the OPC technique.

In general, a pair of optical waves are phase conjugated to each other if their complex amplitude functions are conjugated with respect to their phase factors. Optical phase-conjugate waves can be generated through various nonlinear optical processes (such as four-wave mixing, three-wave mixing, backward stimulated scattering, and others). They can also be generated through one-photon or multi-photon pumped backward stimulated emission processes in a lasing medium. In

[1] Some parts of this review, including the descriptions of OPC principles and a number of selected experimental results, were previously covered in Chapter 9 of the author's recent book [5]. The present review, however, has a broader scope, containing more techniques, the latest progress, as well as additional applications.

many cases, however, one can say that the principles of the major methods for generating optical phase-conjugate waves are based on the intense light-induced holographic gratings and subsequent wavefront reconstruction.

In the area of OPC-related studies, a huge number (more than thousands) of research papers and conference presentations have been published since 1970s. Most of them were based on the degenerate four-wave mixing method in various types of nonlinear media with minor technical modifications. It is impossible and not necessary to mention all (even majority) of them in this review paper. Instead, only a very limited number of publications have been cited here, as they are (i) the original papers with the significance of novelty or innovation, (ii) the earlier studies establishing the basic understanding of related effects or phenomena, and (iii) some selected examples from a large number of quite similar studies.

2. Definitions and features of phase conjugate waves (PCWs)

2.1. Backward degenerate PCW

The term *optical phase conjugation* (OPC) is usually used to describe the wavefront reversion property of a backward propagating optical wave with respect to a forward propagating wave. Suppose there is an input quasi-plane-monochromatic wave with arbitrary phase distortion deviated from an ideal plane-monochromatic wave, i.e.,

$$\mathbf{E}(z,x,y,\omega)=\mathbf{E}(z,x,y)\mathrm{e}^{-\mathrm{i}\omega t}=\mathbf{A}_0(z,x,y)\mathrm{e}^{\mathrm{i}[kz+\varphi(z,x,y)]}\mathrm{e}^{-\mathrm{i}\omega t}. \tag{1}$$

Here, z is the longitudinal variable along the propagation direction, x and y are the radial variables along the beam section, ω is the circular frequency of the optical field, $k=n_0/(2\pi\lambda)$ is the magnitude of the corresponding wave vector, n_0 is linear refractive-index of the propagating medium, $\mathbf{E}(z,x,y)$ is the complex amplitude function, $\mathbf{A}_0(z,x,y)$ is the real amplitude function, and, finally, $\varphi(z,x,y)$ is the phase-distortion function describing the deviation of the real wavefront from an ideal plane wave. If there is a backward propagating wave, which can be expressed as

$$\mathbf{E}'(z,x,y,\omega)=a\cdot\mathbf{E}^{*}(z,x,y)\mathrm{e}^{-\mathrm{i}\omega t}=a\cdot\mathbf{A}_0(z,x,y)\mathrm{e}^{-\mathrm{i}[kz+\varphi(z,x,y)]}\mathrm{e}^{-\mathrm{i}\omega t}, \tag{2}$$

where a is any real constant, then the field $\mathbf{E}'(z,x,y,\omega)$ is defined as backward frequency-degenerate phase conjugate wave of the original forward field $\mathbf{E}(z,x,y,\omega)$.

There are two simple examples for phase conjugate waves. First, if the incident wave is an ideal plane wave with $\varphi(z,x,y)\equiv 0$, after normal reflection from an ideal plane mirror, the reflected wave will be phase conjugate with the incident wave, as shown in Fig. 1(a). Second, if the incident wave is an ideal spherical wave, after normal reflection from an perfect spherical mirror, the curvature of which is the same as that of the incident wave front, the reflected wave will also be phase conjugate with respect to the incident wave, as shown in Fig. 1(b). However, in both cases, if the wavefront of the incident wave or the surface of the mirror is not perfect, the reflected wave can no longer be an ideal phase conjugate wave of the incident wave.

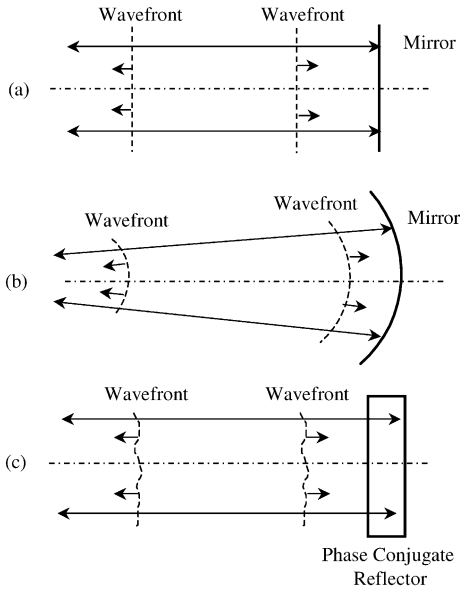

Fig. 1. Three examples of optical phase conjugate waves corresponding to: (a) an ideal plane wave, (b) an ideal spherical wave, and (c) an arbitrarily disturbed wave.

In a more general case, the incident wave may exhibit an arbitrary irregular wavefront; even so, we can still generate its backward phase-conjugate wave from a nonlinear medium by virtue of various nonlinear optical processes. In this case, the nonlinear medium plays the role of a phase-conjugate reflector that creates a backward wave having a reversal wavefront distribution with respect to the propagation direction, as shown schematically in Fig. 1(c).

Fig. 2 schematically depicts the behavior of two different reflected waves backward passing through an inhomogeneous or randomly disturbing medium. One is reflected from an ordinary mirror and the other from a phase conjugate reflector. As shown in Fig. 2(a), an initial plane wave becomes an aberrated wave after passing through the disturbing medium. If we place a plane mirror perpendicularly to the propagation direction of this wave, after reflected from this mirror and passing back through the same disturbing medium, the aberration influence of the medium on the wavefront of the output wave will accumulate. In contrast, as shown in Fig. 2(b), if we replace the plane mirror with a phase-conjugate reflector that creates a phase conjugate wave of the incident beam, then after passing back through the same disturbing medium, the aberration influence will be removed from the final output wave. This is the most important and unusual property of the phase conjugate wave compared to an ordinary reflected wave.

To describe these two different processes shown in Fig. 2, we assume that the initial input wave is an ideal plane wave expressed by

$$\mathbf{E}(z,x,y,\omega) = \mathbf{A}_0(z,x,y)\mathrm{e}^{\mathrm{i}kz}\,\mathrm{e}^{-\mathrm{i}\omega t}, \tag{3}$$

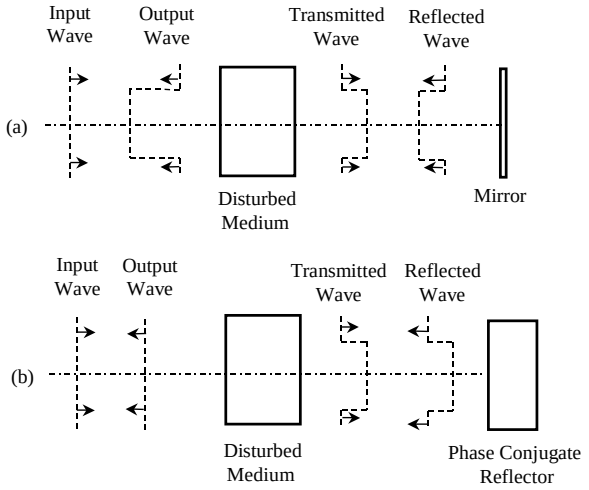

Fig. 2. (a) An ordinary reflected wave backward passes through a disturbed medium, the aberration influence is accumulated; (b) a phase conjugate wave backward passes through the disturbed medium, the aberration influence is removed.

and after passing through a disturbing medium it becomes

$$\mathbf{E}'(z,x,y,\omega) = \mathbf{A}_0(z,x,y)\mathrm{e}^{\mathrm{i}[kz+\varphi(z,x,y)]}\mathrm{e}^{-\mathrm{i}\omega t}. \tag{4}$$

Here $\varphi(z,x,y)$ is a phase function describing the aberration influence on the wavefront from the disturbing medium. If there is an ordinary plane mirror as shown in Fig. 2(a), the reflected wave will be

$$\mathbf{E}''(z,x,y,\omega) = \bar{R}\cdot\mathbf{A}_0(z,x,y)\mathrm{e}^{\mathrm{i}[-kz+\varphi(z,x,y)]}\mathrm{e}^{-\mathrm{i}\omega t}, \tag{5}$$

where $\bar{R}$ is the amplitude reflectivity of the mirror. Then after passing back through the same medium the output wave can be written as

$$\mathbf{E}'''(z,x,y,\omega) = \bar{R}\cdot\mathbf{A}_0(z,x,y)\mathrm{e}^{\mathrm{i}[-kz+2\varphi(z,x,y)]}\mathrm{e}^{-\mathrm{i}\omega t}. \tag{6}$$

In this case the aberration influence for two passes will be doubled.

On the other hand, if there is a phase conjugate reflector, as shown in Fig. 2(b), the reflected wave can be expressed as

$$\mathbf{E}''(z,x,y,\omega) = \bar{R}'\cdot\mathbf{A}_0(z,x,y)\mathrm{e}^{\mathrm{i}[-kz-\varphi(z,x,y)]}\mathrm{e}^{-\mathrm{i}\omega t}, \tag{7}$$

where $\bar{R}'$ is the effective amplitude reflectivity of the phase conjugate reflector. In this case, after passing back through the same disturbing medium the output wave will be

$$\mathbf{E}''' = \bar{R}'\cdot\mathbf{A}_0(z,x,y)\mathrm{e}^{\mathrm{i}[-kz-\varphi(z,x,y)]}\mathrm{e}^{\mathrm{i}\varphi(z,x,y)}\mathrm{e}^{-\mathrm{i}\omega t} = \bar{R}'\cdot\mathbf{A}_0(z,x,y)\mathrm{e}^{-\mathrm{i}kz}\mathrm{e}^{-\mathrm{i}\omega t}. \tag{8}$$

Here, we see an ideal output plane wave, and the aberration influence from the disturbing medium can be entirely removed.

2.2. Backward nondegenerate PCW

So far we assume that the frequency of the reflected wave is the same as that of the incident wave. This belongs to the category of frequency-degenerate optical phase conjugation. Later we will show that a frequency-degenerate PCW can be efficiently produced by using the backward degenerate four-wave mixing method. However, in a more general case, if there is a backward propagating optical field with a frequency ω' different from the frequency ω of the incident wave, which can be written as

$$\mathbf{E}'(z,x,y,\omega') = a\cdot\mathbf{E}^*(z,x,y)\mathrm{e}^{-\mathrm{i}\omega' t} = a\cdot\mathbf{A}_0(z,x,y)\mathrm{e}^{-\mathrm{i}[k'z+\varphi(z,x,y)]}\mathrm{e}^{-\mathrm{i}\omega' t}, \tag{9}$$

then $\mathbf{E}'(z,x,y,\omega')$ is the backward frequency-nondegenerate phase-conjugate wave of an original field $\mathbf{E}(z,x,y,\omega)$ expressed by Eq. (1). In practice, a frequency-nondegenerate backward PCW can be generated by utilizing the following methods: backward nondegenerate four-wave mixing, backward stimulated scattering with certain frequency shift, and backward stimulated emission in a lasing medium. In all these cases, there is a frequency shift between the incident wave and the backward phase-conjugate wave. It can be both experimentally and theoretically proven that the amplitude/phase information carried by the input forward wave of frequency ω can also be restored by the backward PCW with frequency ω'. In this case, however, the quality or fidelity of restored information may undergo certain influence of chromatic aberration when the frequency or wavelength shift is large.

2.3. Forward PCW

Assuming the input wave is described again by Eq. (1), its forward phase conjugate wave can be defined as

$$\mathbf{E}'(z,x,y,\omega) = a\cdot\mathbf{A}_0(z,x,y)\mathrm{e}^{\mathrm{i}[kz-\varphi(z,x,y)]}\mathrm{e}^{-\mathrm{i}\omega t}, \tag{10}$$

where a is any real constant. In this case two related waves propagate along the same direction and have the same frequency, therefore, the wave described by Eq. (10) can also be called the frequency-degenerate forward PCW with respect to the input wave described by Eq. (1).

In a more general case, one can also generate a forward phase conjugate wave with a shifted frequency, such as

$$\mathbf{E}'(z,x,y,\omega') = a\cdot\mathbf{A}_0(z,x,y)\mathrm{e}^{\mathrm{i}[k'z-\varphi(z,x,y)]}\mathrm{e}^{-\mathrm{i}\omega' t}, \tag{11}$$

where $\omega\neq\omega'$. The wave described by above equation can be called the frequency-nondegenerate forward PCW. The physical meaning of a forward phase conjugate wave described by either Eq. (10) or Eq. (11) can be interpreted as following: its wavefront is reversed but the transverse amplitude distribution and propagation direction remains the same as the input wave.

The aberration or distortion influence of the propagating medium on the input wave can be compensated for its forward PCW in two ways, as schematically shown in Fig. 3. Here, it is assumed that the input is an ideal plane wave, that a propagating medium will impose considerable distortion upon the wavefront of the input light

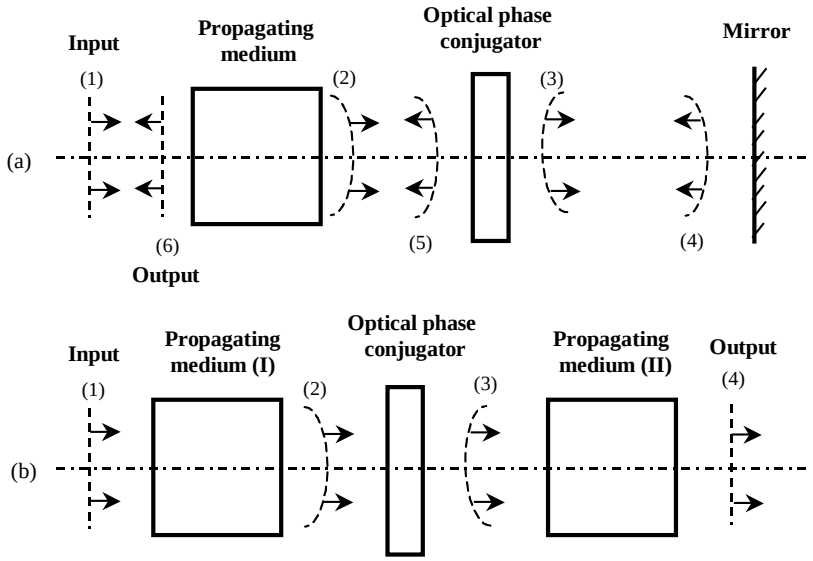

Fig. 3. Forward PCW generation and phase-distortion correction: (a) the combination of an optical phase conjugator with an ordinary mirror reflector; (b) the optical phase conjugator is placed in the middle of two identical propagating systems.

wave, and that an appropriate nonlinear medium is employed as a phase conjugator to produce the forward PCW. In the first way, as shown in Fig. 3(a), the wavefront of the input plane wave is remarkably changed from shape (1) to shape (2) after passing through the propagating medium. When this beam interacts with the phase conjugator, its forward PCW can be generated featuring a reversed wavefront shape (3). After reflection from a perpendicularly placed plane mirror, the forward PCW beam becomes a backward PCW beam with wavefront shape (4). In this case the phase conjugator is supposed to be activated only for a forward input beam but not a backward beam; therefore, after passing through this phase conjugator the backward PCW beam keeps an unchanged wavefront of shape (5). Finally, after passing back through the same propagating medium, the phase distortion influence on the output backward beam can be cancelled, and we will see a perfect wavefront (6) again.

The other way to use a forward PCW to compensate phase distortion influence from propagating media is schematically shown in Fig. 3(b). The feature of this setup is that an optical phase conjugator is placed in the middle of two identical propagating systems that impose the same distortion influence on the propagated light wave. Once again, the optical phase conjugator is employed to produce a forward PCW with wavefront shape (3) of the distorted input wave with wavefront shape (2). After passing through the second propagating system, the phase distortion influence generated by the first system can be finally cancelled. This technical approach is highly useful for long-distance optical fiber communications, where two

spans of the same type of optical fiber can be thought as two identical propagating systems.

3. Methods for producing optical phase conjugated waves (PCWs)

In practice, the backward phase conjugate waves (PCWs) can be produced based on several different physical processes, which include (1) the backward four-wave mixing [9,10], (2) the backward stimulated scattering [11,12], and (3) the backward stimulated emission (lasing) [13,14]. On the other hand, the forward PCWs can be generated based on (i) the forward four-wave mixing [15,16], (ii) the special three-wave mixing in a second-order nonlinear medium [17,18], and (iii) photon-echo processes in a resonant medium [19,20].

3.1. Backward degenerate four-wave mixing (FWM)

The most popular method to generate a backward degenerate PCW is based on the so-called backward degenerate four-wave mixing (FWM), proposed first by Hellwarth in 1977 [9]. In this case, as shown in Fig. 4, a third-order nonlinear medium is illuminated simultaneously with two counter-propagating strong plane waves and a signal beam that has an arbitrary wavefront distortion and different propagation direction. If these three incident waves have the same frequency ω, we may observe a newly generated wave with the same frequency ω but propagating along the opposite direction of the signal beam. The following derivation can simply show that this newly generated wave is the backward frequency-degenerate PCW of the incident signal beam.

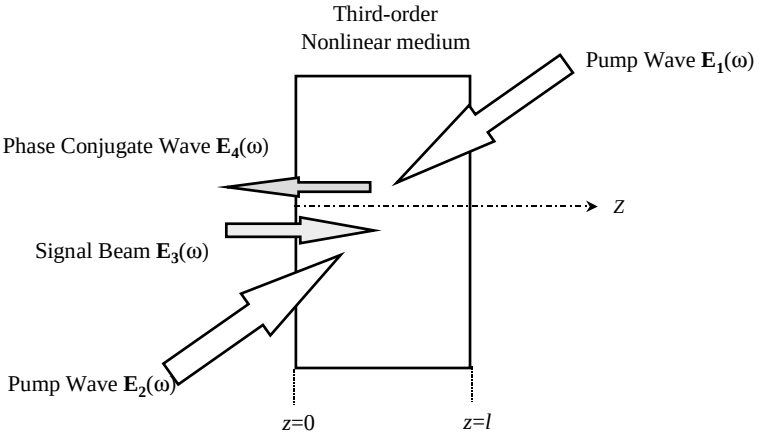

Fig. 4. Phase-conjugate wave generation by degenerate four-wave mixing.

Assuming the signal beam is propagating along the z-axis, the three incident monochromatic waves can be expressed as

$$\begin{aligned}
\mathbf{E}_1(\omega) &= \mathbf{a}_1 A_1(\mathbf{r}) \mathrm{e}^{-\mathrm{i}(\omega t - \mathbf{k}_1 \cdot \mathbf{r})}, \\
\mathbf{E}_2(\omega) &= \mathbf{a}_2 A_2(\mathbf{r}) \mathrm{e}^{-\mathrm{i}(\omega t - \mathbf{k}_2 \cdot \mathbf{r})}, \\
\mathbf{E}_3(\omega) &= \mathbf{a}_3 A_3(z) \mathrm{e}^{-\mathrm{i}(\omega t - k_3 z)},
\end{aligned} \tag{12}$$

where $\mathbf{a}_1$ is a unit vector along the light polarization direction of the ith wave, $\mathbf{k}_1 = -\mathbf{k}_2$ is the wave vector of the one pump wave, k_3 is the absolute value of the wave vector of the signal beam, A_1 and A_2 are the real amplitude functions of the two plane pump waves, and A_3 is the complex amplitude function of the signal wave.

According to the principle of FWM, the fourth coherent wave will be generated through the third-order nonlinear polarization response of the medium. This wave and its corresponding nonlinear electric polarization can be written as

$$\begin{aligned}
\mathbf{P}_4^{(3)}(\omega) &= \varepsilon_0 \chi^{(3)}(\omega, \omega, -\omega) \mathbf{a}_1 \mathbf{a}_2 \mathbf{a}_3 A_1 A_2 A_3^* \, \mathrm{e}^{-\mathrm{i}(\omega t + k_3 z)}, \\
\mathbf{E}_4(\omega) &= \mathbf{a}_4 A_4(z) \mathrm{e}^{-\mathrm{i}(\omega t + k_3 z)}.
\end{aligned} \tag{13}$$

Here the newly generated wave is propagating along the $-z$ direction, and the phase-matching condition is always satisfied because $\mathbf{k}_1 + \mathbf{k}_2 = \mathbf{k}_3 + \mathbf{k}_4 \equiv 0$. As a result of such a process, the signal wave will be amplified while the $\mathbf{E}_4$ wave is created.

For simplicity, it is assumed that the three incident wave are linearly polarized along the same direction (x-axis) and the nonlinear medium is isotropic; therefore, the $\mathbf{E}_4$ wave will also be polarized along the x-axis direction. Under this condition, we can neglect the vector property of the fields and write the third-order nonlinear polarization fields for E_3 and E_4 waves as

$$\begin{aligned}
P_3^{(3)}(\omega) &= \varepsilon_0 \chi_{\mathrm{e}}^{(3)} A_1 A_2 A_4^* \, \mathrm{e}^{-\mathrm{i}(\omega t - k_3 z)}, \\
P_4^{(3)}(\omega) &= \varepsilon_0 \chi_{\mathrm{e}}^{(3)} A_1 A_2 A_3^* \, \mathrm{e}^{-\mathrm{i}(\omega t + k_3 z)}.
\end{aligned} \tag{14}$$

Here, $\chi_{\mathrm{e}}^{(3)} = \chi_{xxxx}^{(3)}(\omega, \omega, -\omega)$ is the effective third-order nonlinear susceptibility value, which is a real quantity for nonresonant interaction or a complex quantity for resonant or near-resonant interaction.

Substituting Eq. (14) into the general expression of nonlinear coupled-wave equations, and assuming the depletion of both, strong pump waves can be neglected within a short interaction length, we then obtain the equation describing the amplitude variation along the z-axis for E_3 and E_4 waves:

$$\begin{aligned}
\frac{\partial A_3^*(z)}{\partial z} &= \mathrm{i}\gamma^* A_4(z), \\
\frac{\partial A_4(z)}{\partial z} &= \mathrm{i}\gamma A_3^*(z),
\end{aligned} \tag{15}$$

where γ in general is a complex coupling coefficient determined by

$$\gamma = \frac{k_3(\omega)}{2\varepsilon_r(\omega)}\chi_e^{(3)}A_1A_2 = \frac{\omega}{2cn_0(\omega)}\chi_e^{(3)}A_1A_2. \tag{16}$$

Here ε_r and n_0 are the linear dielectric constant and refractive index of the nonlinear medium, respectively.

Under the condition that A_1, A_2 and, therefore, γ are approximately constant, the solutions of Eq. (15) can be expressed as [21]

$$\begin{aligned} A_3(z) &= \frac{\cos[|\gamma|(z-l)]}{\cos[|\gamma|l]}A_3(0) - \mathrm{i}\frac{|\gamma|}{\gamma^*}\frac{\sin[|\gamma|z]}{\cos[|\gamma|l]}A_4^*(l), \\ A_4(z) &= \frac{\cos[|\gamma|z]}{\cos[|\gamma|l]}A_4(l) + \mathrm{i}\frac{\gamma}{|\gamma|}\frac{\sin[|\gamma|(z-l)]}{\cos[|\gamma|l]}A_3^*(0), \end{aligned} \tag{17}$$

where A_3 (0) is the initial amplitude of the signal wave on the incident surface of the nonlinear medium. Considering the boundary condition of $A_4(l) = 0$, we obtain the final solutions:

$$\begin{aligned} A_3(l) &= \frac{A_3(0)}{\cos[|\gamma|l]}, \\ A_4(0) &= -\mathrm{i}\frac{\gamma}{|\gamma|}\tan[|\gamma|l]A_3^*(0). \end{aligned} \tag{18}$$

From Eq. (13) we know that the wave E_4 is counter-propagating to the wave E_3; on the other hand, from the second expression of Eq. (18) we know that the complex amplitude $A_4(0)$ is proportional to $A_3^*(0)$ near the incident surface. Therefore, one can conclude that the waves E_4 and E_3 are phase-conjugated to each other and the whole system plays the role of a phase-conjugate reflector. In this case the nonlinear intensity-reflectivity of the system can be determined from Eq. (18) as

$$R = |A_4(0)|^2/|A_3(0)|^2 = \tan^2[|\gamma|l]. \tag{19}$$

If $(\pi/4) < |\gamma|l < (3\pi/4)$, then $R > 1$, indicating an amplification effect of the backward wave E_4. In addition, from the first expression of Eq. (18) we know that $A_3(l) > A_3(0)$, i.e., the signal wave E_3 will be always amplified through the nonlinear medium.

In particular, when the following condition is fulfilled:

$$|\gamma|l = \frac{\pi}{2}, \tag{20}$$

from Eq. (18) we have

$$\frac{|A_4(0)|}{|A_3(0)|} = \infty, \quad \frac{|A_3(l)|}{|A_3(0)|} = \infty. \tag{21}$$

These expressions mean self-oscillation of both waves E_3 and E_4. In reality, this situation will not happen because the solutions given by Eq. (18) are valid only for small signal gain. When the amplitude changes for waves E_3 and E_4 are considerably large, the amplitude functions A_1 and A_2 of the pump beams can no longer be treated

as constants, therefore the solutions expressed by Eq. (18) are not adequate to describe the gain behavior of strong signals. Nevertheless, we still can use Eq. (20) as a rough estimation of the effective interaction length (l_0) for a given nonlinear medium, which is

$$l_0 \approx \frac{\pi}{2|\gamma|} = \frac{cn_0(\omega)}{\omega} \frac{\pi}{\left|\chi_e^{(3)}\right| A_1 A_2}. \tag{22}$$

From Eq. (18) we can see that the greater value of $\left|\chi_e^{(3)} = \chi_{xxxx}^{(3)}(\omega, \omega, -\omega)\right|$ the nonlinear medium has, the stronger reflected wave E_4 it can generate. For nonresonant interaction, $\chi_e^{(3)}$ is a real and small quantity, and consequently, the nonlinear reflectivity R is quite low. To reach a higher nonlinear reflectivity, researchers have to use resonant or near-resonant effects to increase the $\left|\chi_e^{(3)}\right|$ value of the medium [22].

In the above part of this subsection, it is mathematically proven that a PCW can be generated through a special degenerate FWM arrangement in a third-order nonlinear medium. Such a process is essentially related to the four-photon parametric interaction.

In the following part of this subsection, we shall consider a more general interpretation that can explain why the PCW can be generated in such a special FWM arrangement. This model is based on the principle of holography, i.e. two-beam induced volume gratings and the subsequent wavefront reconstruction with the third beam [1,23].

As shown in Fig. 5, there are two counter-propagating plane pump waves (A_1 and A_2) passing through a nonlinear medium, and a signal wave A_3 is incident upon the medium at an angle θ with respect to the pump wave A_1. Under this arrangement the backward propagating wave A_4 can be generated through the reflection from two possible induced gratings. First, let us consider the interference between the two waves A_1 and A_3 that will produce nearly parallel interference fringes along the bisector direction of the crossing angle θ, as shown in Fig. 5(a). Considering that the induced refractive-index change of the medium is proportional to the local light intensity, one may realize that the interference fringes can produce an induced holographic grating within the nonlinear medium. In this case the pump wave A_2 can

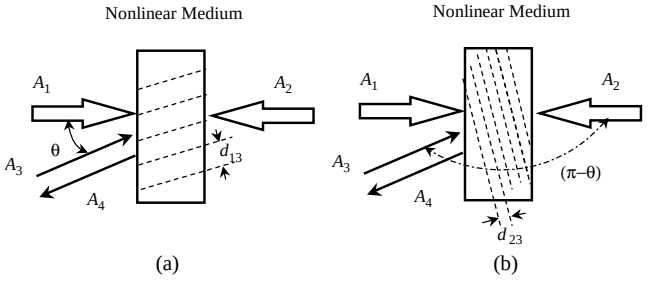

Fig. 5. Schematics describing the generation of a backward phase conjugate wave via induced holographic gratings.

be viewed as a reading beam; during its passing through the induced grating, a diffracted (or reflected) wave A_4 will be created. According to the principle of holography, it is known that this diffracted wave A_4 will restore the spatial information carried by the incident signal wave A_3; in other words, the waves A_4 and A_3 are phase conjugated to each other. To further justify this conclusion we can treat the nonlinear medium as a holographic medium whose transmission function is determined by the interference-induced refractive-index modulation and can be phenomenologically expressed as

$$T \propto (A_1 + A_3)(A_1 + A_3)^* = |A_1|^2 + |A_3|^2 + A_1^* A_3 + A_1 A_3^*. \tag{23}$$

As assumed the waves A_1 and A_2 are two counter-propagating plane waves and $A_2 = A_1^*$, so that the transmitted field of reading wave A_2 will be

$$A_2' \propto TA_2 = TA_1^* = [|A_1|^2 + |A_3|^2]A_2 + A_3(A_1^*)^2 + A_1 A_2 A_3^*. \tag{24}$$

Here on the right-hand side of the equation, the first term proportional to A_2 represents the zero-order diffracted wave that does not involve any spatial information and therefore is not of interest to us. The contribution from the second term that actually involves a phase factor of $\exp[-\mathrm{i}(2\mathbf{k}_1 \cdot \mathbf{r} - k_3 z)]$ can be neglected because its phase-matching condition could not be fulfilled. The third term corresponds to the diffracted wave that involves the spatial information carried by the signal wave A_3 and can be written separately as

$$A_4 \propto A_1 A_2 A_3^*. \tag{25}$$

On the other hand, from Eq. (18) given in the previous subsection we know that under the condition of $|\gamma| l \ll 1$, we have

$$A_4(0) = -\mathrm{i}\gamma l\, A_3^*(0) \propto A_1 A_2 A_3^*(0). \tag{26}$$

Comparing the above two equations we can see that the two different physical models lead to the same conclusion.

As shown in Fig. 5(b), the backward wave A_4 can also be generated through the diffraction of the holographic grating induced by the waves A_2 and A_3. In that case the pump wave A_1 plays the role of the reading plane wave, and the reflected wave A_4 is still phase conjugated to the wave A_3. Although these two gratings can both contribute to the generation of the phase-conjugate wave A_4, the periods of these two grating are different and can be written as (see Fig. 5(a) and (b))

$$\begin{aligned} d_{13} &= \lambda' \left(2 \sin\frac{\theta}{2}\right)^{-1}, \\ d_{23} &= \lambda' \left(2 \cos\frac{\theta}{2}\right)^{-1}, \end{aligned} \tag{27}$$

where λ' is the wavelength of the waves in the medium. It is obvious that these periods of the induced gratings are determined by the corresponding spacing of the interference fringes formed by two appropriate waves.

Till now, all mathematical derivations are based on the assumption that all involved waves have the same frequency and the same linear polarization, and there

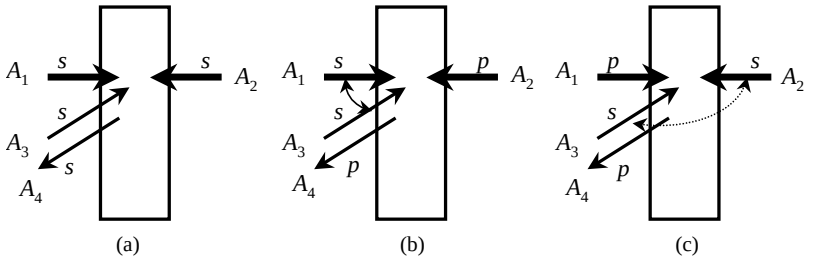

Fig. 6. Backward degenerate FWM under different polarization combinations of the three incident beams: (a) three beams have the same (s) polarization state, (b) A_1 and A_3 beams have the same (s) polarization state, and (c) A_2 and A_3 beams have the same (s) polarization state.

are two gratings giving contributions to the formation of the reconstructed wave, as shown in Fig. 6(a). Now let us consider that the three incident waves have the same frequency, but only two of them have the same linear polarization. Two examples of combinations of polarization states among four waves are shown schematically in Fig. 6(b) and (c).

In the case shown in Fig. 6(b), the waves A_1 and A_3 are both linearly polarized along the direction perpendicular to the plane of paper (the s components), whereas the wave A_2 is linearly polarized in the plane of paper (the p component). It is obvious that only the waves A_1 and A_3 can interfere with each other to produce the phase grating, while the wave A_2 plays the role of the reading wave that creates the phase conjugate wave A_4 with the same polarization state (the p component). Similarly, in the case shown in Fig. 6(c), only the waves A_2 and A_3, which have the same polarization state, can produce the phase grating, whereas the reading wave A_1 and the phase conjugate wave A_4 have the same other polarization state. For more general cases, the polarization states of the three incident waves and the phase-conjugate wave might be more complicated.

3.2. Backward nondegenerate FWM

Next, let us extend our discussions from the degenerate FWM to nondegenerate (or partially degenerate) FWM. In the latter case, two waves have the same frequency (ω_1), while the other two waves have another frequency (ω_2) [24]. Fig. 7 shows two schematics describing the generation of nondegenerate backward PCW via partially degenerate FWM. In the case shown in Fig. 7(a), the pump wave $A_1(\omega_1)$ and signal wave $A_3(\omega_1)$ have the same frequency and the same polarization state, and therefore can produce an induced phase grating. Whereas, the reading wave $A_2(\omega_2)$ with another frequency will create the diffracted wave $A_4(\omega_2)$ through the induced grating. In this case the spatial information carried by the signal wave $A_3(\omega_1)$ can be restored in the wave $A_4(\omega_2)$; in other words, the latter is the frequency-nondegenerate PCW of the former. Similarly, in the case shown in Fig. 7(b) the waves $A_2(\omega_1)$ and $A_3(\omega_1)$ have the same frequency and polarization state and can produce the grating, while the reading wave $A_1(\omega_2)$ with another frequency will

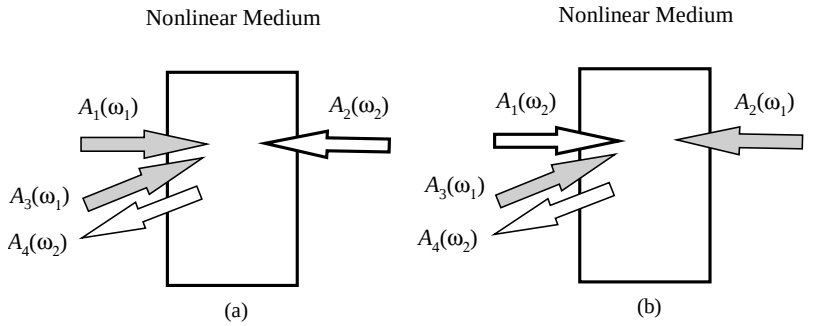

Fig. 7. Schematics describing the generation of the backward nondegenerate PCW via partially degenerate FWM in a nonlinear medium.

create the diffracted wave $A_4(\omega_2)$. In this case $A_4(\omega_2)$ is phase-conjugated with $A_3(\omega_1)$.

The processes described above are essentially the same as that observed when we use two beams of the same frequency to produce a hologram, and then use another beam with a different frequency to read this hologram. In that case the diffracted beam has the same frequency as the reading beam, but the reconstructed spatial structure of this beam may be influenced by the wavelength difference between the recording beams and the reading beam.

In the latter sections we shall indicate that the induced holographic grating model is not only useful to explain the generation of PCW via FWM processes, but also suitable to explain the PCW generation through either the backward stimulated scattering or the backward stimulated emission (lasing) processes.

3.3. Forward FWM

Generally speaking, the forward optical PCW can be generated in a third-order nonlinear medium via specially designed forward FWM arrangement.

Firstly, let us consider the principle of utilizing a forward degenerate FWM setup to generate the degenerate forward PCW [16]. Such an arrangement is schematically shown in Fig. 8, where two strong pump beams (beam 1 and beam 2) of the same frequency are passing through the nonlinear medium with a small intersection angle (θ_{12}) in a horizontal plane. The signal beam 3 with the same frequency is incident nearly in a vertical plane at a small intersection angle (θ_{32}) with respect to beam 2. By adjusting the latter angle and the spatial overlapping in the medium among the three beams until beam 3 is exactly located at a circle, which passes through beams 1 and 2 with an angular diameter of θ_{12} in an observation screen, a newly generated coherent emission beam 4 of the same frequency might be observed at the location symmetrical to that of beam 3 along the circle. Meanwhile, after passing through the nonlinear medium, the intensity of beam 3 is increased. This observation can be well understood if we recognize it as a result of degenerate four-photon parametric processes. This involves the annihilation of two photons from beams 1 and 2, and the

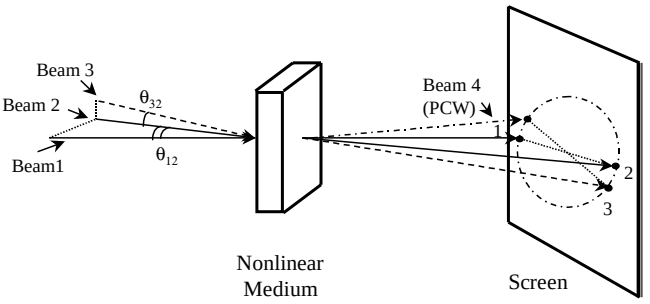

Fig. 8. Forward degenerate FWM setup for generating forward PCW.

simultaneous creation of two photons contributing to beams 3 and 4. The phase-matching condition in this case can be written as

$$\mathbf{k}_1(\omega) + \mathbf{k}_2(\omega) = \mathbf{k}_3(\omega) + \mathbf{k}_4(\omega). \tag{28}$$

Neglecting the depletion of two pump beams within the thin nonlinear medium, we can readily prove that

$$A_4(\omega) \propto A_3^*(\omega), \tag{29}$$

i.e. beam 4 is the forward PCW of the signal beam 3. Here we further extend the definition of forward PCW when two mutually conjugated forward beams may have different propagation directions.

In the arrangement described above, generation of beam 4 can also be explained well by the model of holographic grating. According to this model, the newly generated beam 4 is not only a result of four-photon parametric amplification process, but also is from the refraction of induced gratings. Specifically, there may be two contributions from grating diffraction (or reflection) to the formation of phase-conjugated beam 4: one is from the grating formed by beams 2 and 3 reading by pump beam 1, the other is from the grating formed by beams 1 and 3 reading by pump beam 2. Though it is not easy, it can be done to distinguish the grating contribution from the four-photon parametric contribution. The major difference is that the latter only takes place when three beams arrive at the nonlinear medium at exactly the same time, whereas the former can take place even when one pump beam is delayed with respect to the other, within a certain time interval. In most cases, optical beam-induced gratings can last a certain time period depending on the specific mechanisms of intensity-dependent refractive index changes of the medium. Moreover, if the grating contribution is the dominant mechanism, multi-spot structures may be observed in the screen at a high pump level, owing to a higher-order grating diffraction effect [25].

Next, let us consider how to utilize a nondegenerate forward FWM method to generate the forward PCW. A quite simple experimental approach is shown in Fig. 9(a), where a strong pump beam 1 of frequency ω_1 and a weak signal beam 2 of frequency ω_2 are passing through a third-order nonlinear medium simultaneously

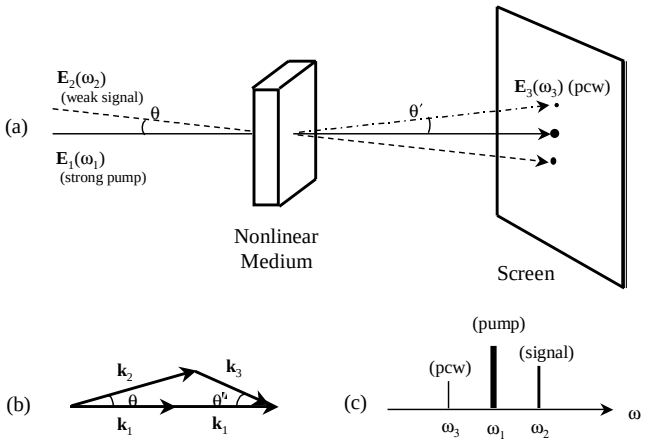

Fig. 9. Forward nondegenerate FWM for generating forward PCW: (a) optical layout, (b) phase-matching, and (c) spectral locations.

with an appropriate intersection angle θ. Under this arrangement a newly generated beam 3 may be obtained in a different forward direction via a noncollinear four-photon parametric process, provided that the following energy conservation and phase-matching conditions are fulfilled:

$$\begin{aligned} 2\omega_1 &= \omega_2 + \omega_3, \\ 2\mathbf{k}_1 &= \mathbf{k}_2 + \mathbf{k}_3. \end{aligned} \tag{30}$$

In this case, it can be easily proven that beam 3 is phase-conjugated with signal beam 2. According to Eq. (30), $\omega_3 = 2\omega_1 - \omega_2 = \omega_1 - (\omega_2 - \omega_1)$, i.e., the signal frequency ω_2 and phase-conjugate frequency ω_3 always exhibit a symmetric distribution with respect to the pump frequency ω_1, as shown in Fig. 9(c). For a given combination of ω_1 and ω_2 as well as the dispersion property of refractive index of the medium, phase-matching angles θ and θ', as shown in Fig. 9(b), can be calculated. In experiments, one may carefully adjust the intersection angle between two incident beams until the phase conjugate beam 3 can be observed. In particular, if $\omega_2 = \omega_1 \pm \Delta\omega_r$ and $\Delta\omega_r$ is the Raman frequency shift of the medium, we will see a Raman-enhanced FWM process, which is essentially similar to CARS (coherent anti-Stokes Raman spectroscopy) or CSRS (coherent Stokes Raman spectroscopy) processes.

Furthermore, if we assume that $\omega_2 \approx \omega_1 \approx \omega_3$ and the refractive-index dispersion is very small within a narrow spectral range covering these three frequencies, then $2n(\omega_1) \approx n(\omega_2) + n(\omega_3)$ and the phase-matching condition shown in Fig. 9(b) can be nearly fulfilled in the same forward direction. This special approach is highly useful for optical fiber communication systems where the forward phase-conjugate waves can be utilized to compensate the chromatic dispersion and nonlinear phase-distortion of a long-distance fiber network. We shall discuss this issue in detail in Subsection 7.3.

3.4. Forward three-wave mixing in a second-order medium

From historical viewpoint, the earliest suggestion for generating PCW based on a special three-wave mixing in the second-order nonlinear crystal was given by Yariv in 1976 [17]. It is well known that such a crystal can be used for second harmonic generation (SHG) at frequency of 2ω pumping with a strong fundamental wave at frequency of ω. For the purpose of PCW generation [18,26,27], one can let the fundamental beam and SHG beam pass through another second-order nonlinear crystal together as shown in Fig. 10. For the second crystal the input fields can be written as (neglecting the polarization property of both beams):

$$\begin{aligned} E_1(\omega) &= A_1(\omega)\mathrm{e}^{\mathrm{i}[\omega t - k(\omega)z]}, \\ E_2(2\omega) &= A_2(2\omega)\mathrm{e}^{\mathrm{i}[2\omega t - k(2\omega)z]}, \end{aligned} \tag{31}$$

which induce a second-order nonlinear polarization wave described by

$$P_3^{(2)}(\omega) = \varepsilon_0 \chi_{\mathrm{e}}^{(2)}(2\omega, -\omega) A_2(2\omega) A_1^*(\omega)\mathrm{e}^{\mathrm{i}(\omega t - [k(2\omega) - k(\omega)]z)}. \tag{32}$$

Here $\chi_{\mathrm{e}}^{(2)}$ is the effective second-order nonlinear susceptibility of the second crystal. Assuming that the phase-matching requirement in this crystal is satisfied, i.e. $k(2\omega) = 2k(\omega)$ or $n(2\omega) = n(\omega)$, then $P_3^{(2)}(2\omega)$ will emit the third optical field of same frequency:

$$E_3(\omega) \propto \chi_{\mathrm{e}}^{(2)} A_2(2\omega) A_1^*(\omega)\mathrm{e}^{\mathrm{i}[\omega t - k(\omega)z]}. \tag{33}$$

Here it is assumed that $E_2(2\omega)$ is a strong pump wave with a negligible depletion within the second nonlinear crystal, and $E_1(\omega)$ is a weak signal beam carrying certain amplitude/phase information. From Eq. (33) one can see that $E_3(\omega)$ is a forward PCW of the signal wave $E_1(\omega)$.

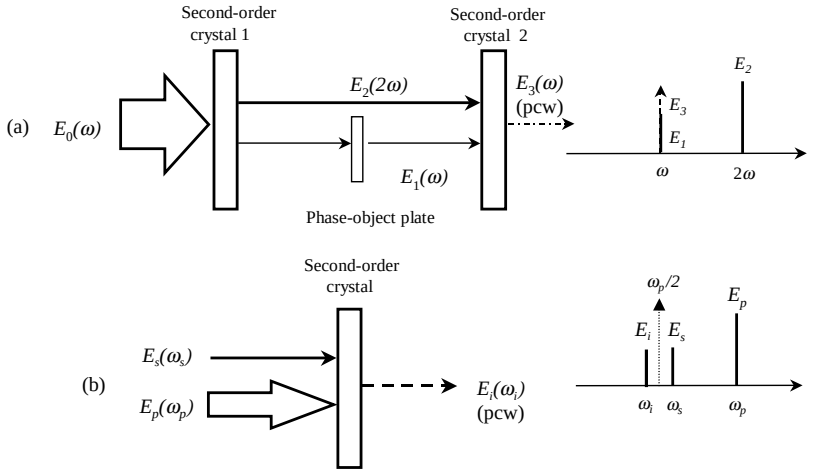

Fig. 10. Three-wave mixing for generating forward PCW in a second-order nonlinear crystal: (a) degenerate difference-frequency generation, (b) quasi-degenerate difference-frequency generation.

In practice, there are two ways to separate the phase-conjugate $E_3(\omega)$ wave from the transmitted signal wave $E_1(\omega)$. The first way is to distinguish one wave from the other by their polarization status. For example, under Type II phase-matching condition in a negative uniaxial crystal, the pump wave $E_2(2\omega)$ and signal wave $E_1(\omega)$ can both be extraordinary rays, while the phase-conjugate wave $E_3(\omega)$ will be an ordinary ray. The second way is to employ a near-degenerate optical parametric amplification process in a second-order nonlinear crystal, where the frequency ω_s of a signal wave is close (not equal) to the half of a strong pump frequency ω_p, i.e. $\omega_s \approx \omega_p/2$. Under similar experimental conditions as that mentioned above, a forward coherent wave can be generated in the crystal at a new frequency of $\omega_i = \omega_p - \omega_s$, as shown in Fig. 10(b). The newly generated (idler) wave $E_i(\omega_i)$ will be phase-conjugated with the signal wave $E_s(\omega_s)$. It should be noted that in this case the spectral positions of these two waves are mirror-symmetric with respect to the value of $\omega_p/2$.

3.5. Backward stimulated scattering

It is well known that upon the excitation of intense and highly directional laser radiation, various types of stimulated scattering can be observed in appropriate scattering media. The most typical of them are stimulated Raman scattering [28], stimulated Brillouin scattering [29], stimulated Rayleigh-wing scattering [30], and stimulated Kerr scattering [31]. Generally speaking, stimulated scattering exhibits the same features as stimulated emission (lasing), such as (i) threshold requirement for pump intensity, (ii) exponential amplification within the gain medium for small signal, (iii) high directionality and brightness of the output coherent beam [5].

From the historical point of view, the earliest observation of the optical phase conjugation (OPC) property was made in the experiment of backward stimulated Brillouin scattering (SBS) in 1972 [11,12]. Since then researchers have found that the similar OPC behavior can also be observed on the backward output of other types of stimulated scattering. Those experimental results showed that the aberration influence imposed on the pump laser beam could be automatically canceled in the backward stimulated scattering beam. In this sense the latter is a nondegenerate backward phase-conjugate wave of the input pump beam, as there is usually a frequency shift between the pump frequency and the backward stimulated scattering frequency.

However, for a long time, there was lack of a clear theoretical model to explain why the similar OPC behavior can be observed via different types of stimulated scattering even though the physical mechanisms for them are totally different. In Section 5, a quasi-collinear four-wave mixing model is suggested as a common mechanism for PCW generation via various backward stimulated scattering processes [32].

3.6. Backward stimulated emission (lasing)

As mentioned in the preceding subsection, there is a remarkable analogy between stimulated scattering and stimulated emission [5]. The only difference between these two processes is that the stimulated emission requires population inversion in a lasing medium, whereas the generation of stimulated scattering does not require such population inversion in a scattering medium. Keeping this analogy in mind, one may expect that the same OPC behavior should also be observed in the backward stimulated emission under proper conditions.

In reality, the superior phase-conjugation property has recently been demonstrated in several two-photon pumped dye lasing systems [14,33]. The results of these studies have shown that under proper experimental conditions the backward stimulated emission from a two-photon pumped gain medium can be a good PCW of the input pump beam. In Section 6, the same quasi-collinear four-wave mixing model, as presented in Section 5, shall be applied to explain why and under what conditions one may produce the phase-conjugate backward stimulated emission from a lasing medium excited with one-photon, two-photon, or even three-photon absorption [34].

4. Studies of PCW generation via four-wave mixing (FWM)

In the area of optical phase conjugation (OPC) research, the majority of experimental studies have been done by the degenerate FWM method. The reason for this is that the principle and visualization of that method is simple and clear, the required laser facilities are relatively inexpensive, and most importantly, a great number and broad variety of materials can be employed as nonlinear optical media for tests. It should be pointed out that a considerable part of those studies has been focused on measuring the nonlinearity of materials themselves, rather than investigating the phase-conjugate properties of backward generated optical beams.

4.1. Experiments

Fig. 11 shows two typical experimental arrangements for observing PCW via backward degenerate FWM. The common feature of these arrangements is that the master beam from a laser source is divided into three beams via appropriate mirrors and beamsplitters. Two of them are used as pump beams and pass through a nonlinear medium in a counter-propagating way, while the third beam containing certain spatial information is incident upon the nonlinear medium with a crossing angle to one of the pump beams. Under these arrangements the backward PCW can be measured in the direction opposite to that of the incident signal beam. To ensure a longer interaction length, the angle between the signal beam and one of the pump beams should be relatively small. In practice, to achieve a higher local intensity the three incident beams are either weakly focused by a lens system or compressed with a reversed beam expander.

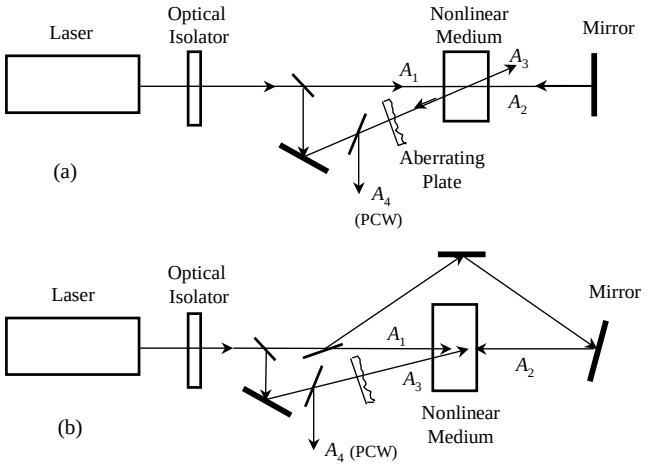

Fig. 11. Two typical experimental setups for PCW generation via degenerate four-wave mixing.

The difference between these two layouts is that, for the former, the backward pump wave is simply provided by a vertically placed mirror, whereas for the latter the two counter-propagating pump waves are provided by an optical ring-path. It is noted that the first arrangement is much simpler than the second. However, the second arrangement is more convenient to examine the influences from various polarization combinations of three incident beams or to change the intensity ratio among them. To eliminate the possible optical feedback from the backward phase-conjugate beam into the laser source, one may put an optical isolator near the output end of the laser device, or simply increase the distance between the laser and the nonlinear medium so that the backward traveling time of the feedback light pulses is longer than the laser-pulse duration.

In experiments the following major aspects have been investigated:

4.1.1. The nonlinear reflectivity R

It is defined as the intensity (or energy) ratio between the incident signal beam and the backward phase-conjugate beam. According to Eqs. (19) and (16), the value of R and related coupling parameter γ can be approximately expressed as

$$R \approx [|\gamma| l]^2 \propto \left|\chi_e^{(3)} A_1 A_2\right|^2 l^2 \propto \left|\chi_e^{(3)}\right|^2 I_1 I_2 l^2. \tag{34}$$

Here, $\chi_e^{(3)}$ is the effective third-order nonlinear susceptibility value of the medium, I_1 and I_2 are intensity values of the two pump waves, l is the effective interaction length in the nonlinear medium, and $|\gamma| l \ll \pi/4$ is assumed.

4.1.2. Fidelity of the phase-conjugate beam

To examine the aberration-correction capability of the phase-conjugate beam, an aberrating plate, which is usually a glass slide etched by hydrofluoric acid solution, can be placed on the incident path of the signal beam. After passing back through

the same aberrating plate, the aberration influence on the phase-conjugate beam might be entirely or partially removed depending on the fidelity of wavefront reconstruction of that beam.

4.1.3. Polarization property of the phase-conjugate beam

As we briefly mentioned in Subsection 3.1, the polarization behavior of PCW is dependent on the polarization states of the three incident beams. Hence, from the study of influences of various polarization combinations among the three input waves, researchers may have a better understanding of the related processes.

4.1.4. Temporal behavior of the pulsed phase-conjugate wave

To test the dynamic response of the PCW generation via FWM arrangements, a short- or ultrashort-pulse laser source should be employed to provide the three input pulsed waves. Letting two writing pulses be incident on the sample simultaneously to produce a phase-grating, and delaying the third reading pulse, one may determine whether the four-photon parametric interaction or the induced phase-grating effect is the main mechanism that leads to PCW generation under given experimental conditions. If the induced grating effect is the major origin, one may further determine what is the dominant mechanism leading to the induced refractive-index changes. There are many mechanisms that can cause intensity-dependent refractive-index changes in nonlinear media, including (a) electronic cloud distortion, (b) intramolecular (Raman) motion, (c) molecular (Kerr) reorientation, (d) opto-electrostriction, (e) photorefractive effect in doped second-order materials, (f) population change, and (g) opto-thermal effect [5]. Different mechanisms have different time-response characteristics, therefore, they can be experimentally identified by measuring the rising and decaying behavior of the induced gratings. Table 1 summarizes the roughly estimated values of rise-time and decay-time for different mechanisms causing refractive-index changes in commonly used nonlinear media.

4.2. Some typical results

The most experimental studies via FWM arrangements can be classified into three broad categories: one is based on nonresonant media, another is based on resonant

Table 1
Estimated values of τ_{rise} and τ_{relax} for different mechanisms causing refractive-index changes

Mechanism	Rise-time (s)	Relaxation-time (s)	Resonant enhancement
Electronic cloud distortion	$\leqslant(10^{-15}$–$10^{-16})$	$\leqslant(10^{-15}$–$10^{-16})$	No
			Yes
Intramolecular motion	$\leqslant(10^{-12}$–$10^{-14})$	$\leqslant(10^{-12}$–$10^{-14})$	Yes
Molecular reorientation	$\leqslant(10^{-12}$–$10^{-13})$	$\leqslant(10^{-11}$–$10^{-12})$	No
Electrostriction	$\geqslant(10^{-9}$–$10^{-10})$	$\geqslant(10^{-9}$–$10^{-10})$	No
			Yes
Population change	$\approx(10^{-10}$–$10^{-13})$	$\geqslant(10^{-8}$–$10^{-10})$	Yes
Opto-thermal effect	$\approx(10^{-8}$–$10^{-10})$	$\geqslant(10^{-3}$–$10^{-6})$	Yes

media, and the third is based on photorefractive materials. Generally speaking, the nonlinear reflectivity is rather low when the nonresonant media are used. In contrast, the nonlinear reflectivity can be significantly increased when an enhancement of the third-order nonlinearity of nonlinear medium is introduced.

4.2.1. Degenerate FWM in nonresonant media

In the earliest experiments of phase-conjugation via FWM, CS_2 liquid was used as a nonresonant nonlinear medium and the three incident beams were the Q-switched visible laser beams. The spatial resolution of the wavefront reconstruction for the phase-conjugate beam could be up to 30 lines/mm [10], and the measured nonlinear reflectivity was $R \approx 10\%$ [35]. To demonstrate the image reconstruction property of the PCW, Fig. 12 shows the photographs of near-field images of the PCW generated via FWM in a CS_2-filled cell [10]. To obtain these photographs, an experimental arrangement like that shown in Fig. 11(a) was used; the uniform signal beam passed through a resolution test target and then was incident upon the nonlinear liquid

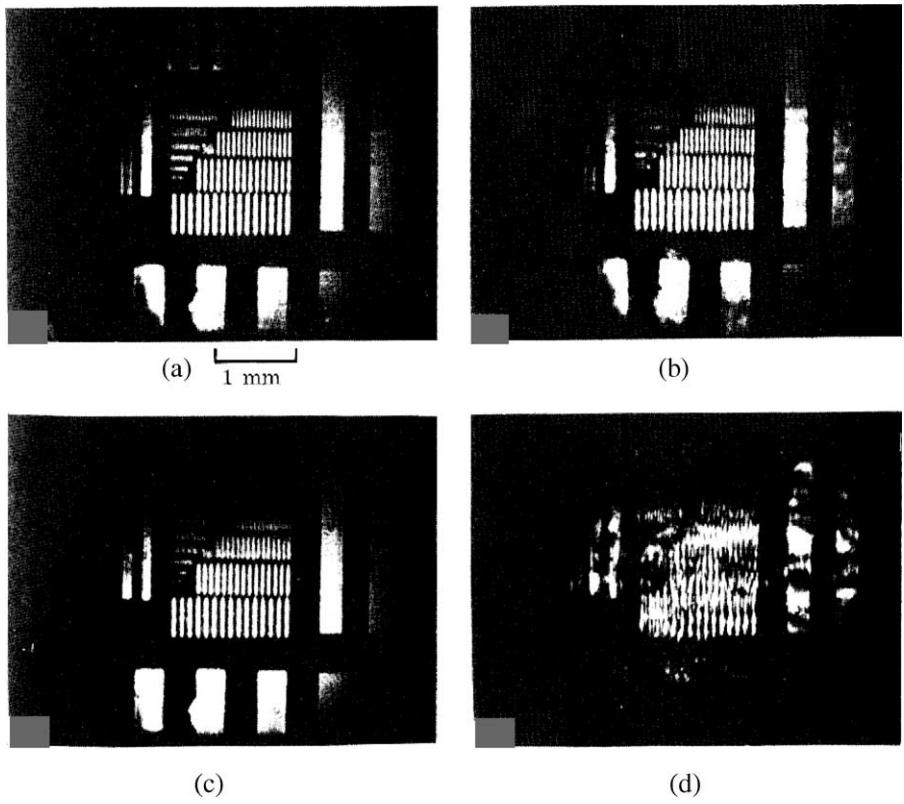

Fig. 12. Photomicrographs of reconstructed images of the phase-conjugate beam via FWM: (a) without aberrator, (b) with aberrator, (c) without aberrator but a rear-mirror misaligned by 0.25 mrad, and (d) with aberrator but the rear mirror misaligned by 0.25 mrad. (From Ref. [10].)

sample. The photographs shown in Fig. 12(a) and (b) were obtained without and with placing an aberrator (a piece of clear glass cut from the side of a bottle) in the path of the incident signal beam, respectively. The photographs shown in Fig. 12(c) and (d) were obtained without and with placing the aberrator on the path, when the rear reflective mirror that provided the backward pump beam was misadjusted by 0.25 mrad vertically. One can see in Fig. 12(c) that the reconstructed image is still clear and just slightly shifted vertically. However, in Fig. 12(d) the image is severely distorted because the backward-generated beam (diffracted from the induced gratings) passed through different portions of the aberrator; therefore the original aberration cannot be corrected.

Some early experimental studies were performed on the semiconductor crystals with 10.6 μm radiation from pulsed CO_2 laser devices. For example, using a polycrystalline Ge bulk sample as the nonlinear medium, the measured nonlinear reflectivity was $R \approx 2\%$ at a pump intensity level of $\sim 1\,\mathrm{MW/cm^2}$ [36]. In a similar experiment, the $Hg_{1-x}Cd_xTe$ alloy was used as a nonlinear medium, and the measured nonlinear reflectivity was $R \approx 9\%$; it was suggested that the nonlinearity of this medium was due to conduction-band nonparabolicity [37].

Another example was the use of the MBBA liquid crystal as a nonresonant nonlinear medium. In that case, the three input beams were from a 694.3 nm Q-switched ruby laser operated on a single longitudinal/transverse mode in a temperature range of $45 \sim 55^{\circ}\mathrm{C}$. The measured maximum nonlinear reflectivity could be as high as $R \approx 230\%$ provided that the two pump beams were circularly polarized in the opposite sense [38].

4.2.2. PCW generation in resonant media

As mentioned before, in order to achieve a higher nonlinear reflectivity, the value of effective third-order nonlinear susceptibility for the medium should be as large as possible. For this reason researchers prefer to choose resonant media in which certain types of resonance enhancements of $\chi_e^{(3)}$ can be utilized.

In early experiments the metal vapors were used as resonant nonlinear media [39,40]. One example was the use of Na vapor pumped by 0.5896 μm laser beams near the D-resonant line position with a detuning of $1.25\,\mathrm{cm^{-1}}$. When the intensities for the pump beam and signal beam were 40 and $0.3\,\mathrm{kW/cm^2}$, respectively, the measured nonlinear reflectivity was as high as $R \approx 10^2$, and the spatial resolution of the phase-conjugate beam was measured to be 4 lines/mm [40]. Fig. 13 shows the measured gain data for the signal beam and phase-conjugate beam as a function of the pump intensity; the theoretical curves shown in the same figure were given by Eq. (18). One can see in Fig. 13 that when the pump intensity was higher than $\sim 30\,\mathrm{kW/cm^2}$, the obvious gain saturation for both beams occurred. In addition, the oscilloscope traces of the input pump pulse and phase-conjugate pulse are shown in the inset of Fig. 13, from which one can see that the pulse duration of the PCW pulse was three times shorter than that of the signal wave pulse.

There are many resonant media that can be utilized for degenerate FWM studies with one-photon resonant enhancement [23,41–46]. In one early experiment, crystals of Nd:YAG, $Cr:Al_2O_3$, $KCl:ReO_4$, etc., were employed for performing FWM, the

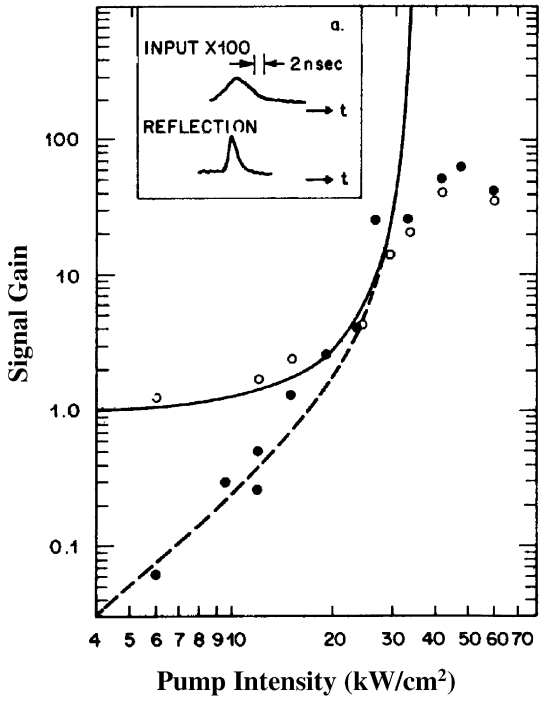

Fig. 13. Measured intensity gain of the phase-conjugate beam (solid points) and transmitted signal beam (open circles) as a function of the pump intensity. The dashed and solid curves are theoretical fits for these two beams. Inset (a): temporal profiles of the input signal pulse and phase-conjugate pulse. (From Ref. [40].)

measured R ranging from 10^{-3} to 10^{-2} [41]. Another interesting medium is SF_6 gas, a saturable absorbing medium for mid-IR radiation; therefore, it can be employed for resonant degenerate FWM. In the experiment the input 10.6-μm beams were provided by a CO_2 laser source, the saturable absorption in SF_6 led to an enhanced refractive-index change, and the measured nonlinear reflectivity was $R = 7\%$ [23,42].

It is expected that semiconductor materials can be used to generate PCW in the IR range with a certain type of resonant enhancement of the third-order nonlinearity. A commonly employed approach is using the near-resonance between the band-gap of a semiconductor medium and the one- or two-photon energy of the input laser beams. There is an example of two-photon enhanced degenerate FWM using Ge crystal as the nonlinear medium. The input radiation provided by a pulsed DF laser source involved multi-lines in the spectral range of $3.6 \sim 4.0\,\mu m$. Since germanium exhibits two-photon absorption at 3.4 μm wavelength, a near-resonant enhancement could be achieved. Under the condition of 3.8 μm single-line excitation at an intensity level of $12\,MW/cm^2$, the measured nonlinear reflectivity was $R = 0.14\%$ [44]. In another experiment, the nonlinear medium was a p-type Si single crystal pumped with 1.06 μm beams from a Q-switched Nd:YAG laser source. Because the

band-gap energy for the Si sample at room temperature is $E = 1.11$ eV, which is close to the single pump photon energy of $h\nu = 1.116$ eV, a near-resonance enhancement can be achieved. For the sample with a residual carrier concentration less than $10^{14}\,cm^{-3}$, the measured nonlinear reflectivity was $R = 105\%$ [45].

It is known that dye solutions or dye-doped solid materials have very strong linear (one-photon) or nonlinear (two-photon) absorption bands in appropriate spectral regions, therefore, they are good candidates for degenerate or partially degenerate FWM studies because of largely enhanced third-order nonlinearity. In these cases, the observed phase-conjugate signals are generated from the diffraction in the induced phase gratings, which are most likely formed via population changes and/or opto-thermal effects. For example, the BDN dye solution is a saturable-absorption medium well known for passive Q-switching at 1.06 μm wavelength. Utilizing this dye solution as a nonlinear medium for the FWM experiment pumped with 1.06 μm laser beams, when the pump intensities were much higher than the saturation intensity value, the measured nonlinear reflectivity was $R = 600\%$ [46].

4.2.3. PCW generation via nondegenerate FWM

Until now we have only described the experimental results based on the degenerate FWM, in which all four waves had the same wavelength or frequency. However, as mentioned in Section 3.2, the PCW can also be generated via nondegenerate (or partially degenerate) FWM processes. In these cases, the two input waves having the same frequency (ω_1) are used to interfere with each other and to produce an induced phase grating, while the third reading beam and the diffracted phase-conjugate wave have another frequency (ω_2) [24,47–51].

As an example, Fig. 14 shows a schematic of the optical layout, employed in the earliest experimental demonstration of partially degenerate FWM [24]. Here a Q-switched and frequency-doubled Nd:YAG laser simultaneously provided two stronger 1.06 μm IR laser beams as well as a weaker 0.53 μm second-harmonic beam. One 1.06 μm laser beam passed through a hole-pattern plate and then interacted with the other 1.06 μm beam to produce a phase grating inside a nonlinear medium. In the mean time, the green laser beam was incident on the medium to read the induced

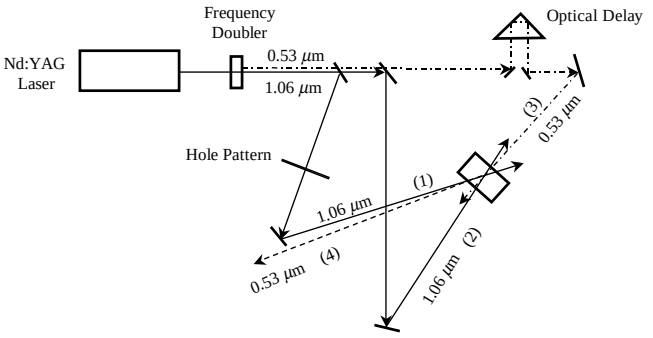

Fig. 14. Optical layout for generating PCW via nondegenerate FWM.

grating and to generate a backward-diffracted beam at the same wavelength of 0.53 μm. In this experiment, more than 14 liquids (including CS_2, water, acetone, benzene, etc.) and an IR filter glass sample were tested, and the observed diffracted beam was found to be a visible replica of the IR signal beam. The image patterns carried by the IR signal beam and restored by the green phase-conjugate beam are shown in Fig. 15. The apparent difference of the image sizes is due to the fact that signal beam was slightly divergent while the backward diffracted beam from the grating was slightly convergent. One can see that there is a fairly good fidelity of the wavefront reconstruction of the replica beam. Moreover, by changing the time delay between the two IR writing beams and the green reading beam, the lifetime of the induced grating can be measured. For most of the tested liquid samples, the results show that the induced gratings could last even more than microseconds. This fact implies that the induced grating is mainly caused by the opto-thermal effect. The thermal grating in the liquid samples might be related to the impurity absorption or two-photon absorption.

Another type of nondegenerate FWM, the so-called Brillouin-enhanced FWM, can also be employed to generate nondegenerate PCW [52–56]. In this approach among the four waves involved, two waves exhibit the same frequency while the frequency difference between two of them should be equal to the backward Brillouin scattering frequency-shift. The possible arrangements of frequency combinations of these four waves are schematically shown in Fig. 16 [55]. In these cases there will be a Brillouin-enhanced traveling-wave grating that plays an essential role in backward PCW generation.

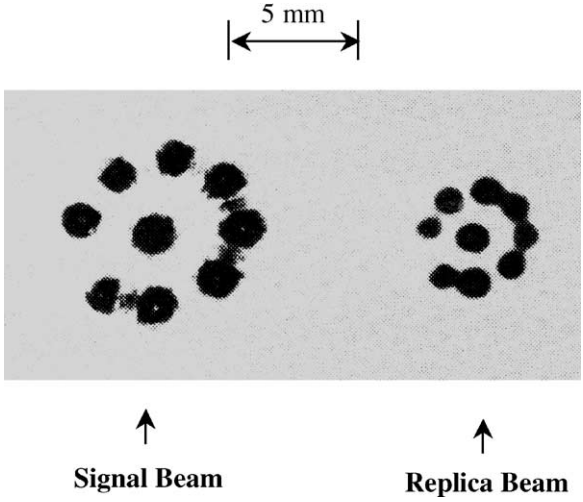

Fig. 15. Images carried by a 1.06 μm signal beam and the 0.532 μm phase-conjugate beam. (From Ref. [24].)

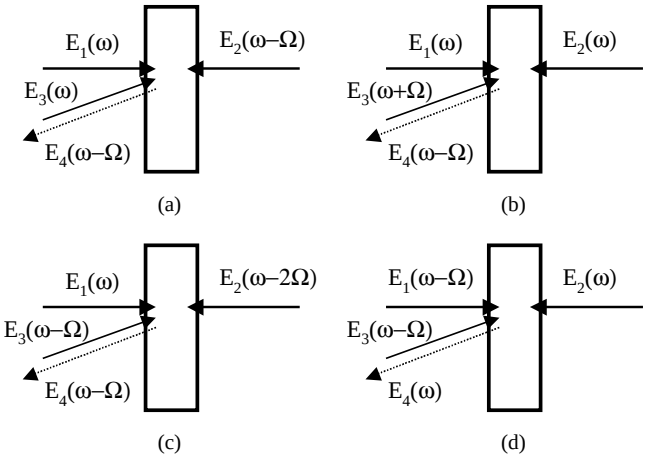

Fig. 16. Brillouin-enhanced FWM with different frequency-combinations for generating PCW with a frequency downshifted (a) and (b), unshifted (c), and upshifted (d).

The significance of using nondegenerate FWM to generate PCW is that:

(i) This is a new technical approach to transfer images from one wavelength to another wavelength with high fidelity,
(ii) The transferred image can be amplified or intensified because it can abstract partial energy from the pump beam via the grating diffraction,
(iii) This process reveals a key insight that explains the phase-conjugate behavior of the backward stimulated scattering and backward stimulated emission (lasing).

4.3. Nonlinear media

The majority of published works in the field of optical phase conjugation and FWM had been based on studying the nonlinear optical properties of a great variety of materials. In order to achieve a higher nonlinear reflectivity or FWM efficiency, a number of forms of resonant enhancement can be involved, including one-photon or two-photon absorption resonance, Raman resonance, Brillouin opto-acoustic resonance, and others. All these types of enhancement may lead to a larger refractive-index change and therefore a higher diffraction (or reflection) efficiency of the induced grating. Unfortunately, however, in many cases the employed resonant enhancements are often accompanied by opto-thermal effects, which might dominate over other mechanisms and provide a poorer reproducibility and less academic significance.

The following is a summary of various types of optical materials commonly used for FWM studies.

(1) *Absorbing liquid and solid materials*. These types of optical media exhibit a strong one-photon or two-photon absorption band covering the

wavelength range of employed laser beams. In most cases the major mechanism causing the induced refractive-index change is either population change or related opto-thermal effect. The typical materials in this category include dye solutions [57–61] or dye-doped matrixes [62–68], impurity-doped glasses [69–75] and crystals [76–79], fullerenes (e.g. C_{60}) related materials [80–82], and liquid crystals [83–86].

(2) *Lasing (gain) media*. Degenerate FWM and phase-conjugation experiments can be achieved in various pumped lasing media, such as Nd:YAG and others [87–92]. In those cases the three incident beams exhibit the same wavelength, i.e. the lasing wavelength of a given gain medium (e.g. 1064 nm for Nd:YAG). One of the major mechanisms producing induced gratings could be the periodic spatial modulation of population distribution in the medium. The advantage of using lasing media as FWM materials might be that the phase-conjugate signal could get additional stimulated amplification through the population inversion systems. The reported nonlinear reflectivity could be up to ~ 2500 for a small signal intensity and multi-pass geometry [88].

(3) *Metal vapors*. Degenerate or near degenerate FWM can be efficiently accomplished in various metal vapors, including Na, K, Rb, Cs, and others [93–99]. Compared with liquid or solid absorbing media, metal atoms in the vapor phase exhibit much narrower absorption line width, therefore the wavelengths of incident laser beams have to be tuned close enough to the chosen spectral transition to reach the necessary resonant enhancement. The reported nonlinear reflectivity can be as high as ~ 300 [100].

(4) *Photorefractive materials*. Degenerate FWM is a common technique to investigate the optical phase conjugation properties of photorefractive materials. It is well known that the photorefractive effect is based on the combination of photoconductivity-induced charge separation and subsequent electro-optic response in a second-order nonlinear medium [101–103]. In this sense the mechanisms of induced refractive-index change are totally different from the above mentioned third-order nonlinear media. For this reason most photorefractive materials used for FWM and phase conjugation studies are impurity-doped inorganic crystals, such as $LiNbO_3$, $LiTaO_3$, $BaTiO_3$, $KNbO_3$, $Sr_{1-x}Ba_xNb_2O_6$ (SBN), $Ba_{2-x}Sr_xK_{1-y}Na_yNb_5O_{15}$ (KNSBN), Bi_{12}(Si, Ge)O_{20}, KH_2PO_4, CdS, GaAs, InP, etc. [104]. In the recent decade, organic crystals and dc-field poled polymer materials have also been employed as novel photorefractive materials for FWM studies [105]. Generally speaking, photorefractive materials can provide a high efficiency light-induced gratings even when using low power cw laser beams in OPC experiments [106,107]. The main disadvantage of this type of nonlinear material for FWM performances is their slow temporal response (usually in $1–10^{-3}$ s range). The details of utilizing photorefractive materials to generate optical phase conjugate waves (PCW) are beyond the scope of this review.

5. PCW generation via backward stimulated scattering

To date, one of the most simple and efficient methods to generate backward PCW is based on various backward stimulated scattering processes, in particular, stimulated Brillouin scattering. In this approach, only a strong and single focused laser beam is needed to pump a given scattering medium, and the backward stimulated scattering beam can be automatically phase-conjugated with the input pump beam, under appropriate experimental conditions. To interpret this special property of the backward stimulated scattering, a quasi-collinear and nondegenerate FWM model can be employed, which may give a clear and straightforward explanation on this property in both qualitative and quantitative ways.

5.1. Phase-conjugation properties of backward stimulated scattering

The earliest observation of the optical phase conjugation effect was made in an experiment of stimulated Brillouin scattering (SBS) in 1972 by Zel'dovich et al. [11] The experimental arrangement used for this type of observation is shown schematically in Fig. 17. Here, the pump source was a single-axial-mode and *Q*-switched ruby laser; the pump beam was passed through an aberration plate and then focused onto the scattering medium. After passing back through the same aberration plate, the spatial structure of the backward SBS could be compared to that of the incident pump beam. In the experiment, the scattering medium was high-pressure CF_6 gas filling in a 94 cm long cell, the divergence of the input $\lambda_0 = 694.3$-nm pump beam was 0.14×1.3 mrad, and after passing through the aberration plate it became ~ 3.5 mrad. If a plane mirror was put in the path of the pump beam and the reflected pump beam was allowed to pass through the aberrator a second time, the beam divergence was increased to ~ 6.5 mrad. Whereas, it was shown that after passing through the same aberrator the backward SBS had nearly the same divergence as the initial pump beam, i.e., the aberration influence was removed. The measured energy-transfer efficiency from the input pump pulse to the backward SBS pulse was $\eta \approx 25\%$ [11]. In another similar early experiment, the scattering medium was CS_2 liquid in a glass cell and the aberration plate was replaced by a poor-quality ruby amplifier rod. The divergence of the initial input pump beam was 0.13 mrad;

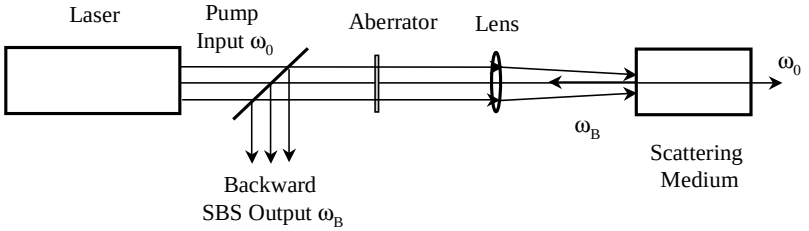

Fig. 17. Experimental arrangement for observing phase-conjugation behavior of backward stimulated Brillouin scattering.

after passing through the amplifier rod it increased to 2.5 mrad. In contrast, after passing through the same amplifier rod the backward SBS exhibited a divergence angle of only ~ 0.15 mrad, and the measured energy transfer efficiency was $\eta \approx 60\%$ [12].

The results of these two experiments showed that the aberration influence imposed on an input pump laser beam could be automatically canceled in the backward SBS beam. In this sense the backward SBS beam is a phase-conjugate wave of the input pump beam. However, during that time period this observation could not be well explained by the known theory of SBS. For this reason, the results did not attract much attention in research community for more than 4–5 years until 1977, when the theories of phase-conjugate wave generation via three-wave and four-wave mixing were suggested [17,9] and experimentally proven [18,10]. Since then studies of PCW generation via backward-stimulated scattering have become more interesting for researchers because of its simplicity and high efficiency.

More importantly, it was found that the PCW could be generated not only by the backward stimulated Brillouin (SBS) process [108–119], but also by other stimulated scattering processes, such as the backward stimulated Raman scattering (SRS) [120–125], stimulated Rayleigh-wing scattering (SRWS) [126–128], and the so-called self-pumped backward stimulated scattering in photorefractive materials [129–134]. Here we shall describe several experimental results that clearly demonstrate the phase-conjugate properties of backward stimulated-scattering beams generated through different scattering mechanisms.

Fig. 18 shows the intensity distributions and photographs of far-field patterns of the original pump beam, the aberrated pump beam, and the aberration-corrected backward SBS beam from CS_2 liquid [108]. The pump beam was a TEM_{00} single longitudinal-mode 694.3 nm pulsed laser beam of 17 ns duration with ~ 0.57 mrad

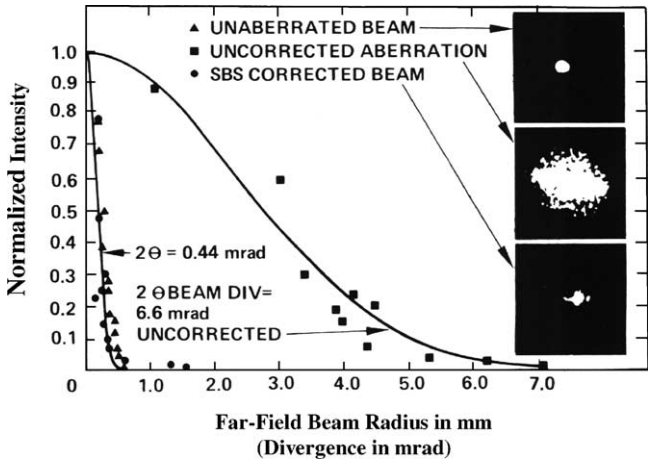

Fig. 18. Normalized far-filed intensity distributions and photographs for the original pump beam, the aberrated pump beam, and the aberration-corrected backward SBS beam. (From Ref. [108].)

divergence angle. After twice passing through an aberrator (a microscope slide etched in hydrofluoric acid), the divergence angle of the pump beam was increased to 6.6 mrad. In contrast, after passing through the same aberrator the backward SBS beam exhibited a much smaller angle of 0.44 mrad; in other words, the aberration was totally corrected.

As another example, Fig. 19 shows the image-reconstruction by a backward stimulated Rayleigh-wing scattering (SRWS) beam from a CS_2-liquid cell pumped with linearly polarized 532 nm laser pulses of 20 ps pulse duration and 15 μJ energy [128]. From Fig. 19 one can see that the influence from the aberrator can to some extent be (not perfectly) removed from the backward SRWS beam.

Finally, the wave-front reconstruction of the backward stimulated scattering beams can also be examined using interference techniques. One experiment based on that method is shown schematically in Fig. 20 [32]. In this case the parameters of the

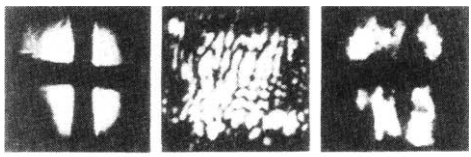

Fig. 19. Near-field image carried by (a) original pump beam, (b) pump beam after twice-passing through an aberrator, and (c) backward SRWS beam after passing through the same aberrator. (From Ref. [128].)

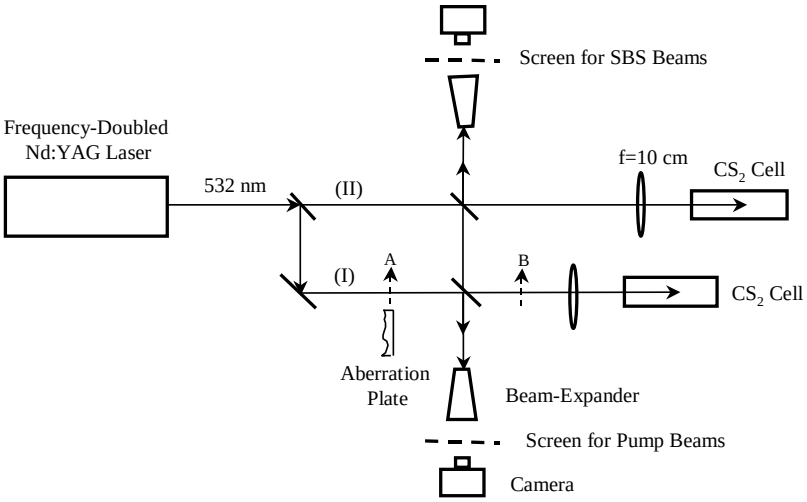

Fig. 20. Experiment for examining the wave-front reconstruction property of backward SBS by two-beam interference method. The aberrator can be inserted in position A or B of the optical path (I). (From Ref. [32].)

pump beam were: wavelength of 532 nm, pulse duration of 10 ns, beam size of 4 mm, and divergence angle of 1 mrad. After passing through a beamsplitter the pump beam was divided into two beams, which were finally focused into two CS_2 liquid cells and to generate their own backward SBS separately.

The example shown in Fig. 20, can produce interferograms formed by the two incident pump laser beams or two backward SBS beams separately. The measured results are shown in Fig. 21 [32]. From Fig. 21(a) one can see that without placing an aberrator, the two-pump-beam interference fringes are quite clear and regular. However, as shown in Fig. 21(b), after one pump beam passed through an aberrator, the interference fringes are severely deteriorated due to the aberration influence. On the other hand, with no aberrator in the optical path, the interference fringes formed by two backward SBS beams are still clear and regular, as shown in Fig. 21(c). This

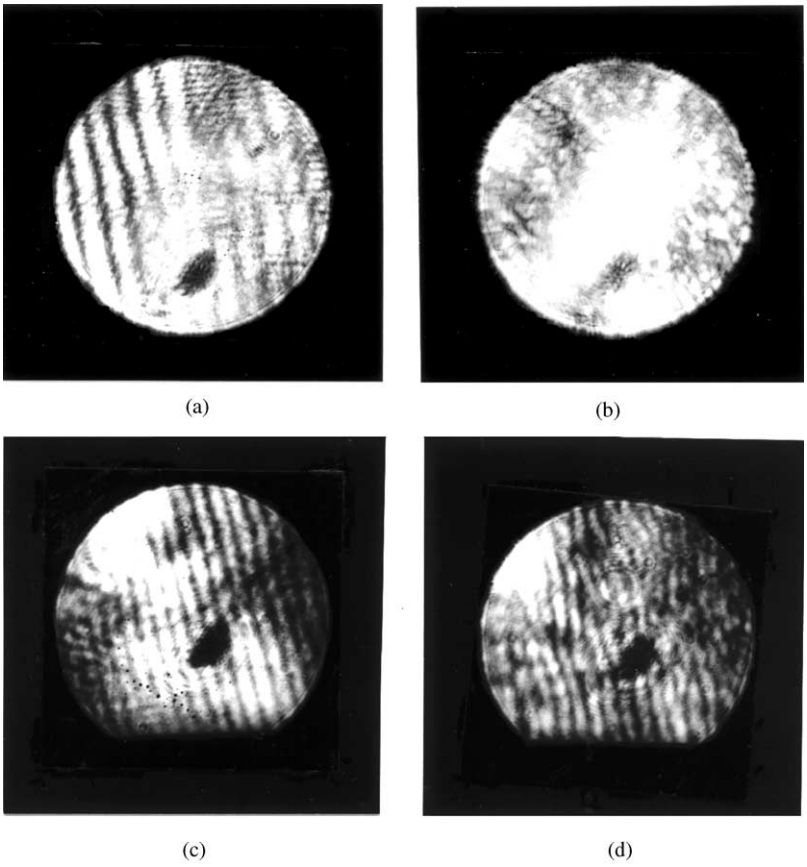

Fig. 21. Interferograms formed by (a) two pump beams without use of an aberrator, (b) two pump beams with the aberrator in position A of the optical path (I), (c) two backward SBS beams without use of the aberrator, and (d) two backward SBS beams with the aberrator in position B of the optical path (I). (From Ref. [32].)

implies that the two backward SBS beams were good replicas of the two pump beams when there was no induced aberration influence. If an aberrator is put in the position B of the optical path (I), the quality of the interference fringes formed by two SBS beams is still fairly good as shown in Fig. 21(d). This is further experimental evidence demonstrating the aberration-correction capability of backward stimulated scattering.

Considering the experimental results described above, we can generally conclude that (i) without or under small aberration influence, the backward stimulated scattering beam can be a nearly perfect replica of the incident pump beam; (ii) under a larger aberration influence the backward stimulated scattering beam can only be an approximate replica of the pump beam. The fidelity of the reconstructed wave front of a backward stimulated scattering beam is determined by many experimental factors, such as the pump intensity level, pump focusing geometry, gain length, type of scattering medium, type of scattering mechanism, frequency-shift range, and the extent of aberration.

5.2. Theoretical explanations: quasi-collinear and nondegenerate FWM model

Though various types of backward stimulated scattering (BSS) can readily be utilized to efficiently generate optical phase-conjugate waves, it has taken quite a long time for researchers to understand the substance of these processes and to give a clear physical explanation without invoking cumbersome mathematical treatments.

A considerable number of the early theoretical papers were published (see, for example, Refs. [2], [135–143] and references therein). Many were based on a phenomenological assumption that there is an exponential gain discrimination (in a factor of 2) between the phase-conjugate portion and non-phase-conjugate portion of BSS; as a result, only the former could get the maximum gain and be effectively amplified in the scattering medium. However, for a long time, there was a lack of a clear theoretical model or physical mechanism to support this assumption. Even ignoring the confusion and discrepancies among some of these papers, most theoretical analyses could not answer a key question: why could only the phase-conjugate portion of the BSS finally become the predominant output? For instance, on the one hand it is known that higher pump intensity is needed to have a better phase-conjugation fidelity for backward stimulated scattering. On the other hand, however, gain saturation will take place under these circumstances; as a result the gain difference between these two portions should be getting smaller, and a worse phase-conjugate fidelity would be expected according to the phenomenological assumption mentioned above. In some existing theoretical analyses both the pump field and BSS field were represented by an infinite series function. In those cases it was extremely difficult to obtain explicit analytical solutions for the nonlinear wave equations.

In addition, we know well that the principle of using degenerate or nondegenerate FWM to produce optical phase-conjugate waves (PCW) is based on the wave-front reconstruction by induced holographic gratings in the nonlinear medium. However, it is also known that the phase-conjugate waves can also be generated from various

types of BSS processes no matter how different the scattering mechanisms are. The latter fact implies that there should be a common origin that determines the phase-conjugation property of any type of BSS and should not depend on the specific scattering mechanism. To find out this common thing, the first insight was made in 1977–1978 when it was suggested that the phase-conjugation nature of BSS might be connected with a special holographic process occurring in the scattering medium [121,122,126]. Later, in 1985–1986, a quasi-collinear FWM model was proposed to explain the phase-conjugation property of the BSS; and this physical model was supported by a rigorous mathematical formulation in the unfocused-beam approximation [144,145]. According to that model, the PCW generation via any type of BSS can be visualized as a nondegenerate or partially degenerate FWM process: the input pump beam contains two waves (E_1 and E_2) of frequency ω_0 while the BSS beam contains other two waves (E_3 and E_4) of frequency ω'. It can be theoretically proven that under certain conditions: $(E_3 + E_4) \propto (E_1 + E_2)^*$ [145,32].

To explain this model more clearly, it is better to invoke Gabor's original idea of holograph. In that case, with a coherent light wave passing through a transparent object (phase object), *the object is assumed to be such that a considerable part of the wave penetrates undisturbed through it, and a hologram is formed by the interference of the secondary wave arising from the presence of the object with the strong background wave*, as clearly described in Ref. [146]. According to this principle, after passing through a phase object, the total optical field can be expressed as a superposition of two portions [146]:

$$U = U^{(i)} + U^{(s)} = A^{(i)}e^{i\varphi_i} + A^{(s)}e^{i\varphi_s} = e^{i\varphi_i}[A^{(i)} + A^{(s)}e^{i(\varphi_s - \varphi_i)}]. \tag{35}$$

Here, $U^{(i)}$ is the undisturbed part of the transmitted field, $U^{(s)}$ is the disturbed part arising from the presence of the object, $A^{(i)}$ and $A^{(s)}$are their amplitude functions, and φ_i and φ_s are the corresponding phase functions.

The Gabor principle is applicable to most phase-conjugation experiments based on BSS. In these cases, as schematically shown in Fig. 22, $E(\omega_0)$ is a quasi-plane

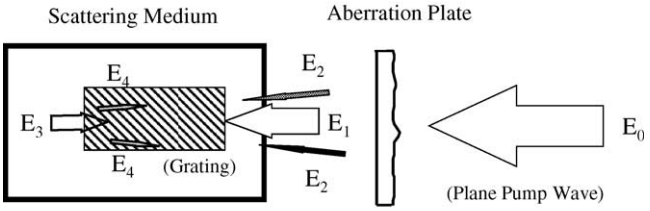

$$[E_3(\omega'<\omega_0) + E_4(\omega'<\omega_0)] = a\,[E_1(\omega_0) + E_2(\omega_0)]^*$$

E_1: Undistorted pump wave;
E_2: Distorted pump wave;
E_3: Initial backward stimulated scattering wave (reading beam);
E_4: Diffracted wave from the induced grating.

Fig. 22. Schematic illustration of the nondegenerate FWM model for the phase-conjugation formation of backward stimulated scattering.

pump wave. After passing through an aberration plate or a phase subject, the pump field manifests itself as a superposition of two portions: a stronger undisturbed wave $E_1(\omega_0)$ and a weaker distorted wave $E_2(\omega_0)$. These two waves interfere with each other in a scattering (gain) medium and create an induced volume holographic grating due to intensity-dependent refractive index changes of the medium. Only the undisturbed pump wave $E_1(\omega_0)$ is strong enough to fulfill the threshold requirement and to generate an initial BSS wave $E_3(\omega')$ that exhibits a regular wavefront as wave $E_1(\omega_0)$. When wave $E_3(\omega')$ passes back through the induced holographic grating region, a diffracted wave $E_4(\omega')$ can be created. Here we see a typical holographic wavefront-reconstruction process: the induced grating is formed by the regular $E_1(\omega_0)$ wave (reference beam) and the irregular $E_2(\omega_0)$ wave (signal beam), the initial backward stimulated scattering $E_3(\omega')$ is a reading beam with a regular wavefront, and the diffracted wave $E_4(\omega')$ will be the phase-conjugate replica of the $E_2(\omega_0)$ wave.

Moreover, the wave $E_4(\omega')$ will experience an amplification with the wave $E_3(\omega')$ together because both waves have the same scattering frequency. In the case of stimulated Brillouin scattering, $\omega_0 \approx \omega'$, it is a nearly degenerate quasi-collinear FWM process. In the case of stimulated Raman scattering, $\omega_0 > \omega'$, there is a partially degenerate and frequency down-converted FWM process. In the case of anti-Stokes stimulated scattering, $\omega_0 < \omega'$, there is a partially degenerate and frequency up-converted FWM process. Based on the explanation described above, one can see a common mechanism (pump field-induced holographic grating) plays the same role for phase-conjugation formation by using either FWM or BSS method. This common mechanism is applicable to all types of backward stimulated scattering processes including stimulated Brillouin, Raman, Rayleigh-wing, Kerr and other scattering, even though the specific scattering mechanisms can be totally different for each other.

Although there is a common ground for PCW generation via conventional FWM or BSS, there is still a remarkable difference between these two processes. For the former, only two waves (the signal wave and the backward diffracted wave) are phase-conjugate to each other; however, for the latter, the sum of the two portions of the BSS beam should be phase-conjugated to the sum of the two portions of the input pump beam. In the next subsection it can be mathematically proven that the latter situation can indeed be realized [145].

5.3. Mathematical treatment in unfocused-beam approximation

According to the proposed quasi-collinear and partially degenerate FWM model of the BSS process, after passing through an aberration plate the total input pump field can be expressed by the sum of two portions:

$$E_p(\omega, z) = [A_1(z) + A_2(z)\mathrm{e}^{\mathrm{i}\theta(z)}]\mathrm{e}^{-\mathrm{i}(\omega t + kz)}. \tag{36}$$

Here, A_1 and A_2 are the real amplitude functions of the undistorted portion and the distorted portion of the pump field, θ is a phase change function, the pump field is propagating in the $-z$ direction, and k is the magnitude of the wave vector. For

simplicity, we assume that the original input pump field is an ideal monochromatic and uniform plane wave before passing through the aberration plate. Thus A_1 and A_2 are only the functions of z. Here θ represents the deviation of wavefront of the distorted portion from an ideal plane wavefront.

Based on the picture illustrated in Fig. 22, the total backward stimulated scattering field can also be expressed by a sum of two portions:

$$E'(\omega', z) = [A'_1(z) + A'_2(z)\mathrm{e}^{-\mathrm{i}\theta'(z)}]\mathrm{e}^{-\mathrm{i}(\omega' t - k' z)}. \tag{37}$$

Here, A'_1 is a real amplitude function of the initial BSS wave (reading beam), A'_2 is a real amplitude function of the diffracted wave through FWM or grating diffraction, and θ' is the relative phase change function between the A'_1 and A'_2 waves. In Eq. (37) it is assumed that the initial backward stimulated scattering is also an ideal plane wave; this assumption is supported by experimental results without using an aberration plate. In the steady-state condition, A_1, A_2, θ and A'_1, A'_2, θ' are independent of time t.

In a small-signal approximation, the initial BSS wave experiences an exponential gain described by

$$A'_1(z) = A'_1(0)\mathrm{e}^{gA_1^2 z/2}, \tag{38}$$

where g is the exponential gain factor due to stimulated amplification from the scattering system.

As a result of interaction among the three waves of A_1, A_2 and A'_1, the fourth wave of A'_2 can be generated through the mechanism of FWM or grating diffraction, and it will get the further stimulated-scattering amplification as A'_1 does. The wave equation obeyed by the diffracted wave of $E'_2 = A'_2\,\mathrm{e}^{-\mathrm{i}\theta'(z)}\,\mathrm{e}^{-\mathrm{i}(\omega' t - k' z)}$ can be written as

$$\nabla^2 E'_2 - \frac{n_0^2(\omega')}{c^2}\frac{\partial^2 E'_2}{\partial t^2} = \mu_0 \frac{\partial^2 P_2^{(3)}}{\partial t^2}, \tag{39}$$

where n_0 is the linear refractive index, μ_0 is the permeability of free space, and $P_2^{(3)}$ is the third-order nonlinear polarization contribution to the wave E'_2, which can be expressed as

$$P_2^{(3)} = \varepsilon_0 \chi_{\mathrm{e}}'^{(3)} A_1 A'_1 A_2\,\mathrm{e}^{-\mathrm{i}\theta(z)}\mathrm{e}^{-\mathrm{i}(\omega' t - k' z)}. \tag{40}$$

Here, $\chi_{\mathrm{e}}'^{(3)}$ is a formally introduced effective third-order nonlinear susceptibility value. If we only consider the gain behavior of the amplitude A'_2, $\chi_{\mathrm{e}}'^{(3)}$ can be viewed as a pure imaginary quantity, i.e. $\chi_{\mathrm{e}}'^{(3)} = \mathrm{i}\chi_{\mathrm{e}}''^{(3)}$, where $\chi_{\mathrm{e}}''^{(3)}$ is a real quantity. Substituting Eq. (40) into Eq. (39) and using slowly varying amplitude approximation leads to

$$\begin{aligned} &\frac{\partial A'_2}{\partial z} + \frac{A'_2}{2k'}\nabla^2\theta' = \frac{k'\chi_{\mathrm{e}}''^{(3)}}{2} A_1 A_2 A'_1 \cos\delta\theta, \\ &\frac{\partial \theta'}{\partial z} + \frac{1}{2k'}(\nabla\theta')^2 = \frac{k'\chi_{\mathrm{e}}''^{(3)}}{2} A_1 A_2 A'_1 \frac{1}{A'_2}\sin\delta\theta, \end{aligned} \tag{41}$$

where

$$\delta\theta = \theta - \theta'. \tag{42}$$

In the small aberration approximation and under the high single-path gain condition, i.e.

$$gA_1^2 z \gg 1, \tag{43}$$

one can finally obtain the following approximate solutions:

$$A_2'(z) = \frac{A_2}{A_1} A_1'(z) = \frac{A_2}{A_1} A_1'(0) \mathrm{e}^{gA_1^2 z/2},$$
$$\delta\theta(z) = \theta(z) - \theta'(z) \Rightarrow 0, \tag{44}$$

The physical meaning of the second equation above is that while the wave $A_2'(z)$ is getting stronger through the exponential gain, its wavefront is getting closer to the wavefront of the wave A_2.

Based on Eqs. (37), (38) and (44), the final solution of the total backward stimulated scattering field is

$$E' = \frac{A_1'(0)}{A_1} \mathrm{e}^{gA_1^2 z/2} [A_1 + A_2 \, \mathrm{e}^{-\mathrm{i}\theta(z)}] \mathrm{e}^{-\mathrm{i}(\omega' t - k' z)}. \tag{45}$$

Comparing this expression with the following expression for the total input pump field

$$E_\mathrm{p} = [A_1 + A_2 \, \mathrm{e}^{\mathrm{i}\theta(z)}] \mathrm{e}^{-\mathrm{i}(\omega t + kz)}, \tag{46}$$

we see that the output backward stimulated scattering field can be a phase-conjugate replica of the input pump field, provided that the high gain condition of Eq. (43) is satisfied. In practice, this requirement can be achieved by increasing either the effective gain length or the pump intensity level.

It should be pointed out that the theoretical treatment described above is based on the small-aberration influence. Experimental results have shown that under a small aberration influence, the output backward stimulated scattering can be a good phase-conjugate wave of the input pump field.

So far, we have not considered the influence of the difference between ω and ω' or between k and k' on the phase-conjugation property of the BSS beam. This influence resembles that a case when someone creates a hologram with two beams of frequency ω and then reads this hologram with another beam of frequency ω'. In this case the size or position of the reconstructed image might be slightly changed.

Finally, the aforesaid theoretical treatment is based on the near-plane wave approximation. However, in most experiments, the pump beams are focused into the scattering medium. In that case we should invoke the Hermite–Gaussian beam approximation, and the mathematical treatment will be somewhat lengthy [32]. Nevertheless, similar conclusions can be reached for the circumstance of a focused pump field, and the high gain of stimulated scattering is still the basic requirement. However, in this case it can be derived that a nearly perfect phase-conjugate wave can only be obtained for the small aberration influence; under the larger aberration influence the fidelity of wavefront reconstruction of the BSS beam will deteriorate.

6. PCW generation via backward stimulated emission (lasing)

In many aspects, the stimulated scattering process is similar to the stimulated emission process, as indicated in Sections 3.5 and 3.6. Therefore, it is not surprising that under appropriate conditions, backward stimulated emission may exhibit the same phase-conjugation property as backward stimulated scattering.

6.1. Single-pass stimulated emission from a two-photon pumped (TPP) lasing medium

In recent years, considerable effort has been devoted to developing frequency-upconversion lasers. There are two major approaches to achieve this goal: one is based on the sequential multi-step one-photon excitation, the other on the direct two-photon excitation. In both cases one could generate a lasing output of wavelength shorter than the pump wavelength. A number of newly synthesized organic dyes have allowed two-photon-pumped (TPP) cavity lasing in dye solutions and dye-doped solid systems using various optical configurations [147–151]. In all those cases, the single-pass gain could be so high that even without using any cavity mirrors or window reflection, highly directional and frequency-upconverted stimulated emission can be obtained in both forward and backward directions once the input pump intensity is higher than a certain threshold level. Furthermore, it is shown that similar to backward stimulated scattering, TPP backward stimulated emission also possesses the property of optical phase conjugation [14,33].

As a typical example, the lasing medium can be a solution of a new dye ASPI [14]. It exhibits a strong one-photon absorption band centered at ~ 500 nm with a 90 nm bandwidth, but no linear absorption in the spectral range of 0.62–1.5 μm. The pump source was a Q-switched Nd:YAG pulsed laser, which provided the laser output with a wavelength of 1064 nm, divergence angle of ~ 1.5 mrad, pulse width of ~ 11 ns, and a repetition rate of 5 Hz. The pump beam was focused via an $f = 20$ cm lens onto the center of a 1 cm-long liquid cell filled by the ASPI dye solution in benzyl alcohol with a concentration of $d_0 = 0.06$ M/l. To avoid the possible TPP cavity lasing formed by the two parallel windows of the liquid cell, the normal of the windows was tilted to $\geqslant 10^\circ$ with respect to the input pump beam. The peak wavelength position and the spectral width of the stimulated emission are ~ 616 and ~ 11 nm, respectively. Finally, the net energy-conversion efficiency from the absorbed pump energy to the backward stimulated emission should be corrected to $\eta' \approx 10\%$ [33].

6.2. Phase-conjugation properties of TPP backward stimulated emission

In general, the phase-conjugation property of a backward-going beam with respect to a forward-going beam can be fully determined by comparing the far-field and near-field patterns of these two beams. The same methods can also be used to examine the phase-conjugation nature of the TPP backward stimulated emission. Fig. 23 shows two typical experimental arrangements that can be used to measure the far-field pattern and the near-field image of the backward stimulated emission separately.

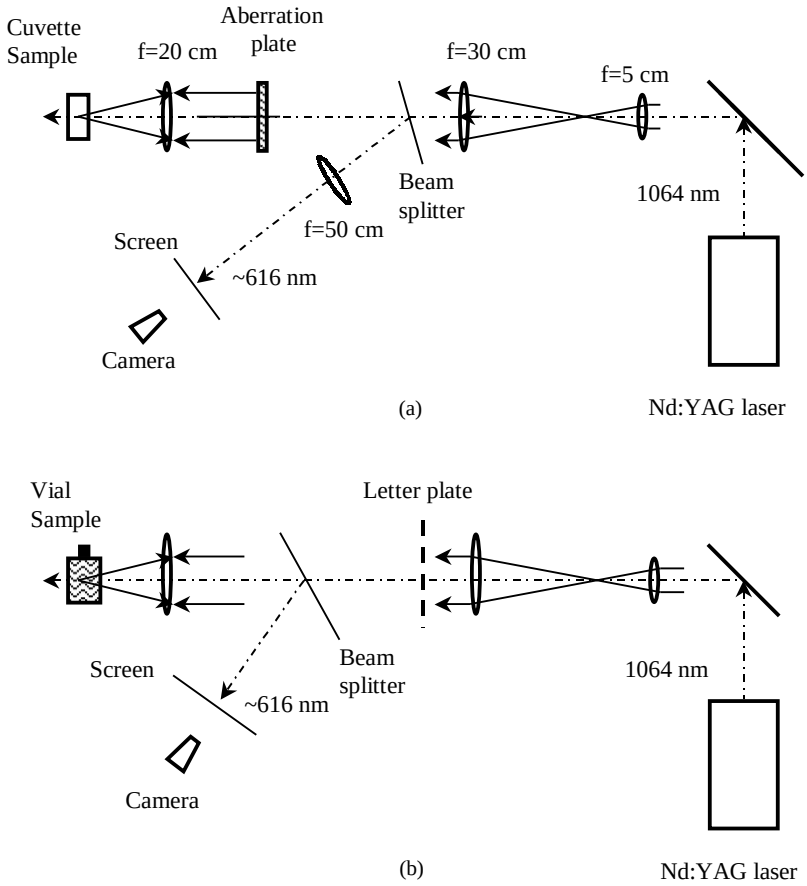

Fig. 23. Experiment for demonstrating phase-conjugation properties of the TPP backward stimulated emission: (a) configuration for the far-field measurement and (b) configuration for the near-field image measurement.

In the case shown in Fig. 23(a), an aberration plate was placed in front of an $f = 20$ cm focusing lens. The backward stimulated emission was recollimated by the same $f = 20$ cm lens, passed through the aberration plate, and then focused via an $f = 50$ cm lens onto a display screen. In this way, the far-field distribution of the backward stimulated emission can be measured and recorded with a digital CCD camera.

In another case (shown in Fig. 23(b)), the dye solution cell was a glass vial. In this case the glass wall of the vial itself played the role of aberration plate. To demonstrate the image-reconstruction ability of the backward stimulated emission, a letter-printed plate, made by printing a black letter of 10 mm size on a transparent film, was placed between the beam splitter and the beam expander. If the backward

stimulated emission had the phase-conjugate nature, a clear image of the letter plate should be observed on the screen.

In an experimental arrangement as shown in Fig. 23(a), the measured divergence angles (FWHM) for the pump beam, forward stimulated emission and backward stimulated emission were ~ 0.25, 0.23, and 0.23 mrad, respectively, without insertion of an aberration plate. The corresponding far-field distributions for these three beams are shown in Fig. 24(a).

To test the aberration-compensation capability of backward stimulated emission, an aberration plate was inserted in the path of the input pump beam, which was a glass slide etched by hydrofluoric acid solution, and could cause either a 0.8–0.9 mrad irregular aberration influence by one pass or a 1.6–1.8 mrad aberration influence by two passes. The results under this condition are shown in Fig. 24(b). These results show that, after passing back through the aberration plate, the aberration influence is almost entirely removed from the backward stimulated

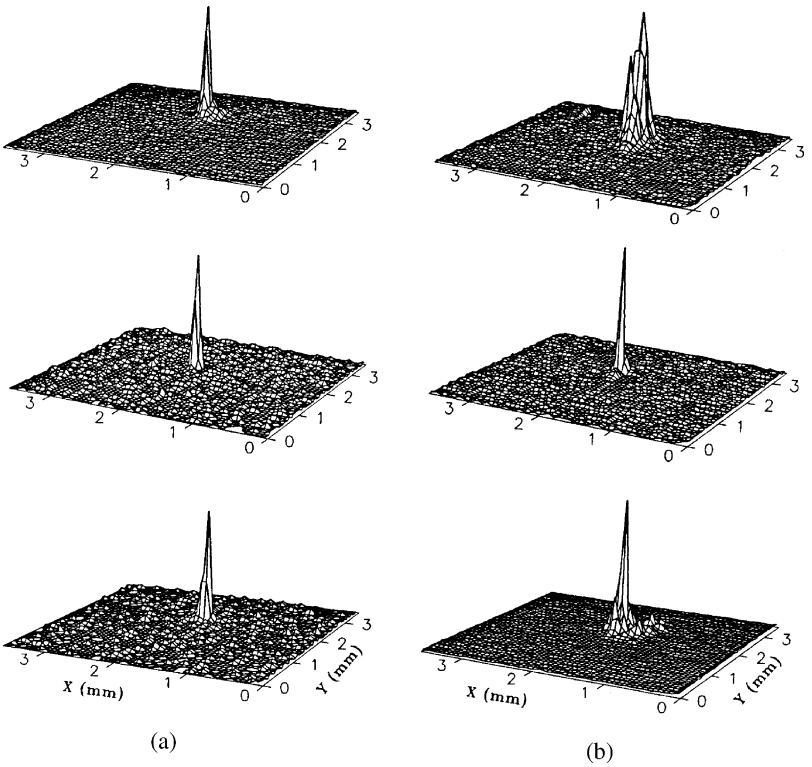

Fig. 24. Normalized far-field intensity distributions for the input pump beam (upper), the backward stimulated emission beam (middle), and the forward stimulated emission beam (bottom): (a) without placing an aberrator and (b) with placing an aberrator. The display resolution is ~ 0.07 mm or ~ 0.13 mrad. (From Ref. [14].)

emission; whereas there is a remarkable aberration influence remaining in the bottom regions of the far-field profile for forward stimulated emission.

A similar experiment was carried out based on the setup shown in Fig. 23(a), with no aberrator in place but, replacing the dye solution-filled cuvette with a dye-solution-filled glass vial, so that the glass wall of the vial played the role of an aberration plate. Fig. 25(a) shows the resultant far-field pattern of the original incident 1064 nm-pump beam with a divergence angle of ~ 0.25 mrad. Fig. 25(b) shows the far-field pattern of the transmitted pump beam after passing through a glass vial filled with pure solvent (benzyl alcohol). The beam divergence angle is increased to 0.7×1.2 mrad, and the unsymmetrical distribution of the aberrated pattern was due to the quasi-cylindrical shape of the wall of the glass vial. Fig. 25(c) shows the far-field distribution of the TPP backward stimulated emission from an ASPI solution-filled vial at a pump level of 1.7 mJ, where the beam divergence angle of the backward stimulated emission is ~ 0.25 mrad and the aberration influence from the vial's wall is almost completely removed. Lastly, Fig. 25(d) shows the far-field distribution of the forward stimulated emission from the same ASPI solution-

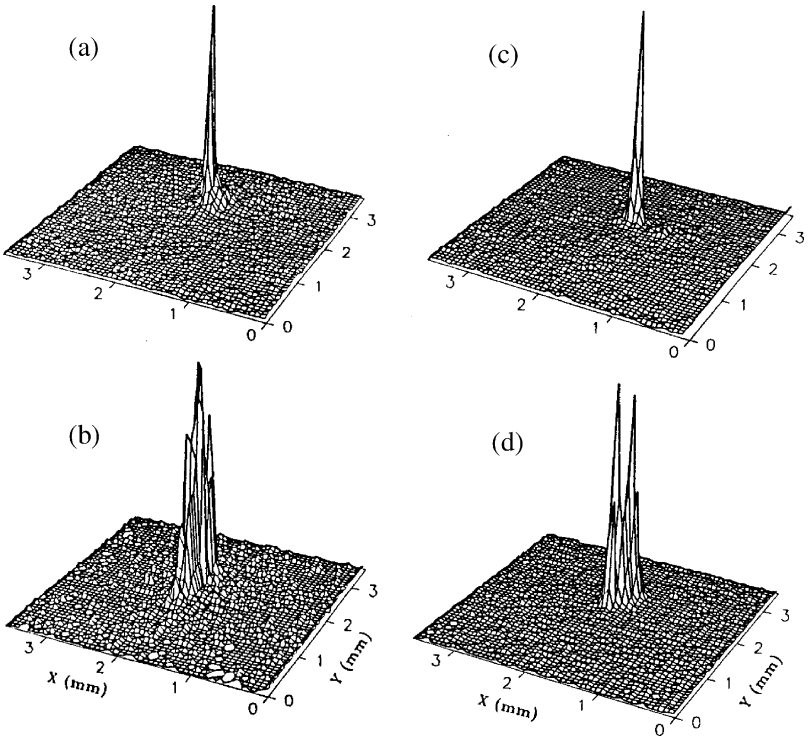

Fig. 25. Normalized far-field profiles for (a) the input 1064 nm pump beam, (b) the transmitted pump beam through a glass vial filled with pure solvent, (c) the backward ~ 616 μm stimulated emission, and (d) the forward stimulated emission from a dye-solution filled glass vial. Here 1-mm dimension corresponds to 2 mrad divergence angle. (From Ref. [33].)

filled vial at the same pump level of 1.7 mJ, where the severe aberration influence is rather obvious.

Another important feature is that the original image carried by the input pump field can be reconstructed by the backward stimulated emission beam after passing through the aberrator or a disturbing medium. To demonstrate this feature, the experimental setup shown in Fig. 23(b) was employed. In that case, a letter-printed transparent film was placed between the $f = 30$ cm lens and the beam splitter, and the gain sample was the same ASPI solution-filled glass vial. After reflection from the beam splitter, the collimated TPP backward stimulated emission was directly projected onto a paper screen, and then the image message recorded with an ordinary camera.

Fig. 26(a) shows a photograph of the incident 1064 nm pump beam after passing through the letter plate. This image is obtained by illuminating the pump beam on an IR sensor card. Fig. 26(e) shows a photograph of the forward upconverted stimulated emission collimated via an $f = 20$ cm lens, the original image message is totally lost owing to the influence of aberration from the vial wall. Fig. 26(f) shows a photograph of the backward stimulated emission of ~ 616 nm wavelength, where one can see that the original image is basically reconstructed by the backward stimulated emission after passing through the vial wall.

To compare the capability of image reconstruction for the backward stimulated emission with that for the backward stimulated scattering, Fig. 26(b) shows a photograph of the backward SBS from an acetone-filled glass vial. In this case, the experimental setup was the same except that the 1064-nm pump beam was replaced by a frequency-doubled Nd:YAG laser beam of 532 nm wavelength. In addition, Figs. 26(c) and (d) show the forward- and backward SRS from a benzene-filled vial at the first-order Stokes wavelength of the 992 cm^{-1} Raman mode pumped with the same 532 nm laser beam. Once again, only the backward stimulated scattering shows the image restoration capability. From that comparison one can see that these three methods have shown nearly the same near-field restoration performance under the experimental conditions described above [33].

6.3. Explanations for the phase-conjugation nature of backward stimulated emission

The appropriate experimental conditions for generating backward single-pass stimulated emission can be summarized (i) the pump beam should be a focused laser beam, (ii) there should be a high single-pass gain in the gain medium, (iii) the interaction length should be much longer than the beam size, and (iv) the aberration influence should not be too large. Based on these considerations, one may realize that the physical model and theoretical treatment used to explain the phase-conjugation property of the backward stimulated scattering are also applicable to the case of backward stimulated emission [34].

The starting point is still the Gabor principle or the associated quasi-collinear and nondegenerate (or partially degenerate) FWM process occurring in a TPP lasing medium. This process is schematically shown in Fig. 27. Here, $E_0(\omega)$ is a quasi-plane pump wave, and after passing through an aberration plate or a disturbing medium, it

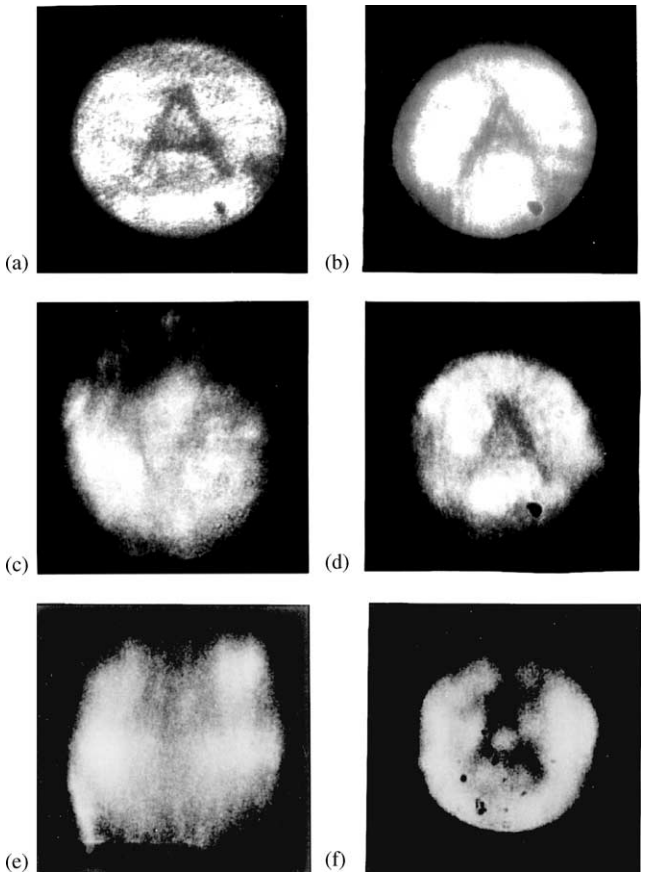

Fig. 26. Near-field images carried by (a) 532 nm (or 1064 nm) input pump beam, (b) the backward stimulated Brillouin scattering from an acetone-filled vial, (c) and (d) the forward and backward stimulated Raman scattering from a benzene-filled vial, (e) and (f) the forward and backward two-photon pumped stimulated emission from an ASPI dye solution-filled vial. (From Ref. [33].)

manifests itself as a superposition of two portions: a stronger, undisturbed wave $E_1(\omega)$ and a weak and distorted wave $E_2(\omega)$. After further passing through a focusing lens, these two waves interfere with each other in the focal region inside the gain medium and create an induced volume holographic grating. Only the wave $E_1(\omega)$ is strong enough to fulfill the threshold requirement and to generate an initial backward stimulated emission wave $E_3(\omega')$ at a new wavelength. As the $E_3(\omega')$ wave backward passes through the induced-holographic grating region, a diffracted wave $E_4(\omega')$ is created, which will be the phase-conjugate replica of the wave $E_2(\omega)$ and undergo further amplification together with the wave $E_3(\omega')$. In the case of two-photon excited stimulated emission, $\omega < \omega'$, there is a partially degenerate and frequency-upconverted FWM process. It can be theoretically proven that under appropriate conditions, the total backward field $(E_3 + E_4)$ can be the

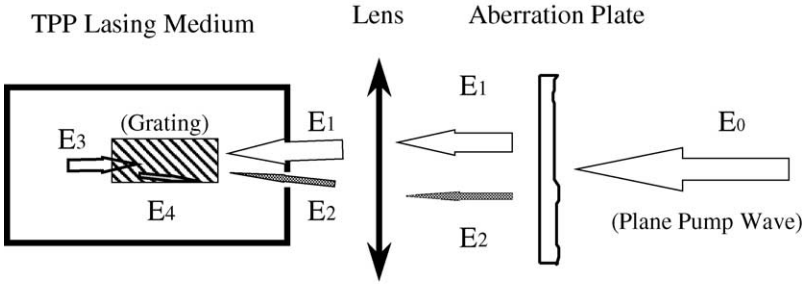

Fig. 27. Schematic illustration of the Gabor holographic principle and partially degenerate FWM process associated with two-photon pumped backward stimulated emission. (From Ref. [34].)

phase-conjugate replica of the total input pump field $(E_1 + E_2)$, i.e. [34]

$$(E_3 + E_4) \propto (E_1 + E_2)^*. \tag{47}$$

Let us consider a TPP isotropic gain medium. Assuming both of the pump field and the stimulated emission field are linearly polarized along the x-axis, the pump field-induced refractive index change experienced by the emission field can be expressed as

$$\Delta n(\omega') = \frac{1}{2n_0(\omega')}\chi_e^{(3)}(-\omega';\omega',-\omega,\omega)|E(\omega)|^2, \tag{48}$$

where $n_0(\omega')$ is the linear refractive index, $\chi_e^{(3)} = \chi_{xxxx}^{(3)}$ is the matrix element of the third-order nonlinear susceptibility tensor, and $E(\omega)$ is the amplitude function of the incident pump field. In the focal region inside the gain medium the local intensity of the pump field, $I(x,y,z,\omega) \propto |E(x,y,z,\omega)|^2$, can be very high with a spatial characteristic intensity fluctuation due to the interference between the two parts (disturbed and undisturbed) of the pump field. Therefore, an intensity-dependent holographic grating can be formed based on the mechanism described by Eq. (48). As a result, a given reading wave of frequency ω' will create a diffracted wave at the same frequency ω' through this induced volume holographic grating inside the gain medium.

According to the proposed physical model, the fidelity of phase conjugation of the backward-stimulated emission is dependent on the modulation depth of the induced holographic grating, and the latter is determined by the magnitude of the induced refractive-index change. In the case of two-photon pumped stimulated emission from a dye solution, the induced refractive-index change can be greatly enhanced owing to

the two-photon absorption related resonance and/or the frequency-upconverted one-photon emission related resonance.

6.4. Phase-conjugation properties of one-photon pumped backward stimulated emission

Based on the studies described above, one would expect that a similar phase-conjugation property may also be observed for backward stimulated emission from a one-photon pumped lasing medium, provided that the optical pump beam is a focused laser beam and no optical cavity is involved. Indeed, there was an early experimental report that briefly described the observation of the partial phase-conjugation behavior of backward superradiance generated in a one-photon pumped Rhodamine-6G dye solution. After backward passing through an aberration plate, only (10–20)% of the backward superradiance exhibited the phase-conjugation property [13].

After the discovery of the superior phase-conjugation property for the backward stimulated emission from a two-photon pumped lasing medium, a further study on a one-photon pumped lasing medium has been pursued under the similar experimental condition [152]. In this case, the gain medium is a solution of a new lasing dye Pyrromethene 597 (PM-597) or this dye-doped polymer rod, pumped by 532 nm and nanosecond laser pulses. The experimental setup was basically the same as that shown in Fig. 23. For both the solution sample in a regular quartz cuvette and the rod sample in a glass vial, when the input pump energy rose above the threshold level, one-photon-pumped highly directional and stimulated emission of ~ 573 nm wavelength could be observed in both the forward and backward directions. This behavior was quite similar to that observed in two-photon pumped experiments [148,150].

In order to examine the phase-conjugate property of the backward simulated emission, an aberration plate could be placed between the beamsplitter and the focusing lens when a dye-solution filled cuvette was used. In the case of using a dye-doped rod filled glass vial, the glass wall of the vial played the role of an aberrator. Under these experimental conditions, the far-field measurement results show that most of these aberration influences are removed from the backward stimulated emission beam rather than from the forward emission beam. Obviously, this is the evidence of a fairly good phase-conjugate property related to the backward stimulated emission via one-photon pumping.

6.5. Phase-conjugation via three-photon pumped backward stimulated emission

Very recently, the first observation of three-photon pumped stimulated emission was reported [153]. In this work the gain medium was a novel organic chromophore (APSS) dissolved in dimethyl sulphoxide (DMSO). Upon the excitation of $\sim 1.3\,\mu$m ultrashort pump pulses, highly directional and visible (~ 553 nm) stimulated emission could be observed in both forward and backward directions. The stimulated emission wavelength was shorter than 1/2, and longer than 1/3, of the pump wavelength.

A further study has shown that the similar three-photon pumped stimulated emission can also be observed in the other chromophore (ASPI) solution in DMSO, pumped by $\sim 1.5\,\mu m$ ultrashort pulses, and the stimulated emission wavelength is $\sim 610\,nm$ [154].

In the latter work, the phase-conjugate property of backward stimulated emission is demonstrated by its capability of removing the dynamic aberration influence of the disturbing gain medium. It was experimentally found that there was a random temporal fluctuation within the beam area for forward stimulated emission, whereas the transverse intensity distribution was more uniform and temporally stable for the backward stimulated emission beam. The much fluctuating behavior of the forward stimulated emission can be explained considering the thermal disturbing effect occurring in the gain region of the solution sample pumped with intense IR pulses at 1 kHz repetition rate. The three-photon absorption and subsequent molecular radiationless transitions may cause a considerable local temperature-change, leaving an irregular and temporally fluctuated aberration influence on the forthcoming pump and forward stimulated emission pulses. By contrast, if we assume that the backward stimulated emission exhibits an optical phase conjugation property, the above-mentioned thermal aberration influence might be automatically removed to a certain extent. To prove that assumption a photodiode detector was placed in the central region of the near-field pattern for each of these two beams separately. The output of this photodiode is connected with a gated integrator. Fig. 28 shows the measured results under 1 kHz pump excitation with three different integrating rates. From Fig. 28 one can see that the spatial and temporal fluctuations for the forward beam are obviously greater than the backward beam, and the relatively smaller fluctuation behavior of the backward stimulated emission indicates its phase-conjugation property.

7. Applications of OPC

The major requirements for OPC techniques are (i) the simplicity and compactness of optical arrangements, (ii) a lower requirement for input (pump) beam intensity levels, (iii) a higher energy- or intensity-conversion efficiency from the input pump beam to the output phase-conjugate beam, (iv) faster temporal response of the nonlinear medium, and (iv) a better wave-front restoration fidelity for the phase-conjugate beam.

According to the above criteria, the most useful and efficient methods for generating phase-conjugate waves (PCW) seem to be backward stimulated scattering, backward stimulated emission, four-wave mixing (FWM), and special three-wave mixing in second-order nonlinear media.

7.1. Potentials of OPC applications

In general, OPC is a highly useful and very unique approach to exploring the nonlinear optical properties of various materials and to investigate different physical

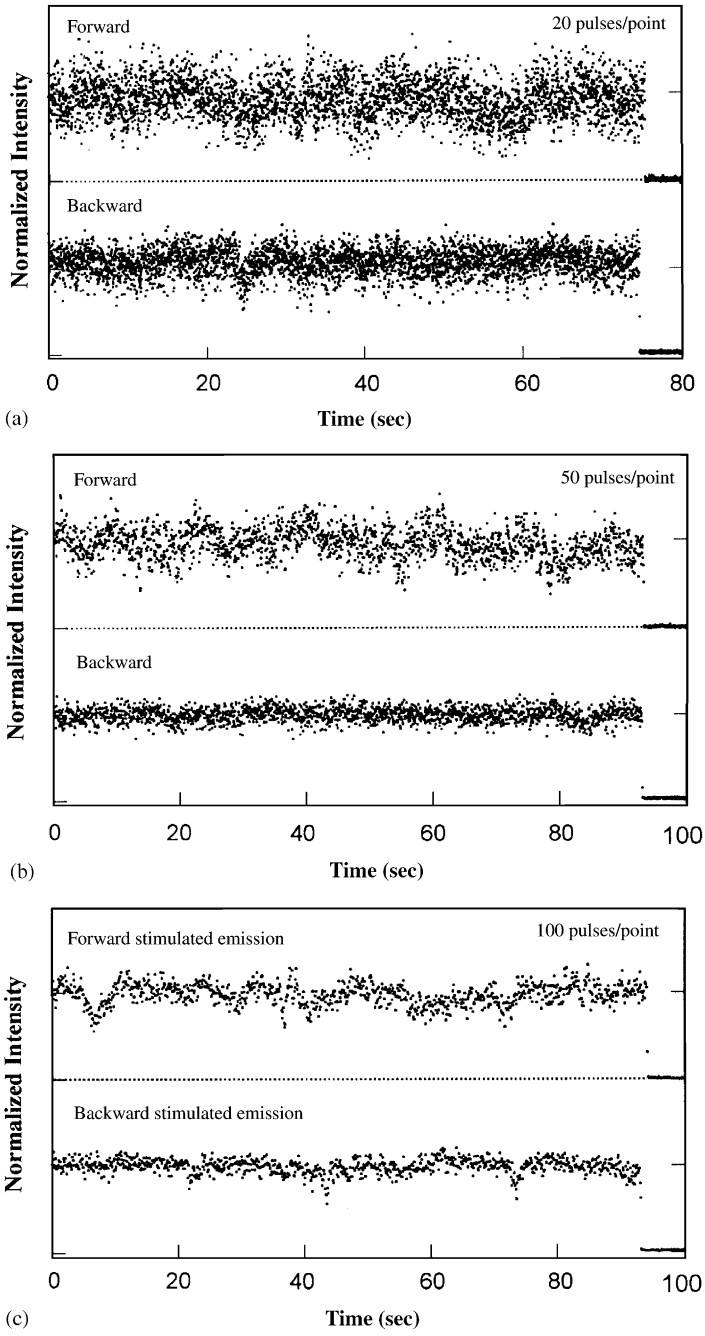

Fig. 28. Intensity fluctuation behavior measured by an ~ 0.3 mm opening photodiode in the near-field pattern for the forward and backward stimulated emission beams at three different averaging rates. (From Ref. [154].)

processes occurring in those media under the action of strong coherent optical fields. On the other hand, based on their wavefront-reconstruction or phase-distortion compensation capability, the OPC techniques are especially useful for many different applications [1–8,106,107].

Fig. 29 shows some distinctive examples of practical and potential applications of phase conjugate waves.

7.1.1. Laser oscillator systems with a phase-conjugate reflector

As shown in Fig. 29(a), the rear mirror of a laser cavity is replaced by a phase conjugate reflector that generates a phase-conjugate feedback wave. Comparing to conventional laser oscillators, this design is capable of producing laser output with a higher brightness and smaller beam divergence, because the aberration influence of the gain medium can be automatically compensated.

7.1.2. Laser amplifier systems with a phase-conjugate reflector

It is known that the dimensions of the gain medium in a laser amplifier are considerably larger than that in a laser oscillator. A larger volume of the gain medium usually yields a greater aberration influence on the lasing beam. For this reason the divergence and brightness of the output beam from the amplifier will be limited by the optical quality of the gain medium itself. If we adopt a phase conjugate reflector in connection with the amplifier and let the reflected laser beam backward pass through the amplifying medium once again, as shown in Fig. 29(b), the aberration influence from the gain medium will be removed, and a high-brightness output laser beam can be obtained.

7.1.3. Laser target-aiming and auto-focusing systems

Another special application of optical phase conjugate waves is related to laser-based target-aiming systems. The principles of these systems are schematically shown in Fig. 29(c) and (d). For the case shown in Fig. 29(c), the lasing medium emits a superradiant emission beam that exhibits a larger beam divergence and can easily cover the target, the partially reflected beam from the target surface can pass through the lasing medium twice with the use of a phase-conjugate reflector. After two-pass amplification the high-power and backward output laser beam will be focused automatically on the target. This kind of technique can be applied for those purposes, such as laser fusion reaction, laser trapping, laser-based rangefinder, lidar, laser target locking, and laser microfabrication.

7.1.4. Laser weapon systems

Laser target-aiming principle can be perfectly applied to laser weapon systems for destroying either static or high-speed flying targets. A similar but modified design is shown in Fig. 29(d), where an auxiliary low-power laser device is to provide a broad illumination beam to cover the target, so that the partially reflected beam from the target surface will pass through a laser amplifier twice by invoking a phase-conjugate reflector. In this case, the aberration influences from irregularity of the target surface, from inhomogeneity of the gain medium, and from disturbance in

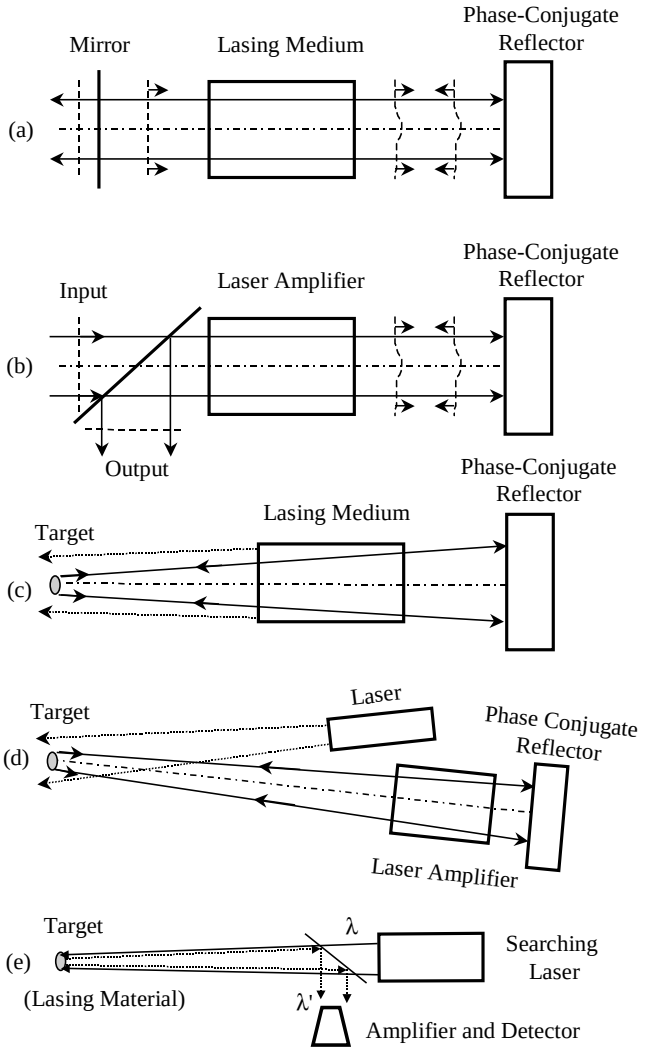

Fig. 29. (a) High-brightness laser oscillator with a phase conjugate reflector as the rear cavity-reflector, (b) high-brightness two-pass laser amplifier with a phase conjugate reflector, (c) laser target-aiming and auto-focusing system, (d) laser target-aiming and weapon system, (e) laser identification and rescue system.

transmission medium can be automatically removed, and the total energy of the amplified laser beam can be efficiently focused on the target to destroy it.

7.1.5. Laser identification and rescue systems

A suggested laser-based friend-or-foe identification system is schematically shown in Fig. 29(e), in which a cooperative lasing material-made target is equipped on an aircraft, a warship, or an armored vehicle. Utilizing a laser aiming system to search

this cooperative target and then focusing the pump laser beam on it, the induced backward and phase-conjugate stimulated emission beam with special wavelength will go back to the laser searching system, to be detected and identified. Obviously, this technique can also be used for rescue of military persons when a radio-silence has to be kept.

7.2. Some examples of OPC application studies

In this subsection we shall give some specific examples of OPC application studies.

7.2.1. Laser oscillator/amplifier systems using stimulated Brillouin scattering mirror

Stimulated Brillouin scattering (SBS) [155–159] is the most efficient technique applied to laser oscillator/amplifier systems, to provide phase-conjugate feedback and to compensate the aberration influence of lasing media. As the frequency-shift of SBS is much less than the gain width of a given lasing medium, the reflected phase-conjugate beam can be effectively amplified. In fact, a Brillouin cell plays the role of phase-conjugate mirror. The cell may contain a transparent liquid (such as CS_2, CCl_4, acetone, n-hexane, cyclohexane, Freon) system, or a high-pressure gas (such as SF_6, CH_4, N_2) system. The nonlinear reflectivity can be higher than 70–80%.

7.2.2. OPC-associate nonlinear spectroscopy

Four-wave mixing based OPC [100,160–163] can be employed as a novel spectroscopic method to investigate the energy state structure, spectral width, and population relaxation of a given resonant nonlinear medium.

7.2.3. OPC-associate phase-locking

Photorefractive crystal based OPC elements, such as the so-called double phase-conjugate mirror, can be utilized to couple two separate laser systems and to keep a synchronized phase relationship between them [164–169]. The laser phase-locking can also be implemented using Brillouin-enhanced FWM method [56]. In addition, the OPC technique is also specially useful for two-beam optical trapping purpose [170].

7.2.4. OPC-associate interferometry

Combining OPC technique with the conventional interferometry [171,172] may provide at least two benefits. One is making the rigorous optical alignment much easier, the other is reducing the environmental disturbance on the measurements.

7.2.5. OPC-associated optical data processing

OPC technique [173–178] will be more useful for optical data recording/reading [173,174], transmission through disturbing medium [96,175,176], memories [177], and filtering [178].

7.3. Midway OPC for fiber communication systems

In regard to recent OPC applications, the most significant breakthrough is the adoption of OPC in upgraded long-distance optical fiber communication systems. It is well known that to achieve high-bit-rate data transmission through a super-long optical fiber network, the following two requirements are essentially important. First, suitable optical wavelengths should be chosen at which the transmission loss in the fiber network is minimized. Second, an appropriate multichannel mechanism should be employed, either in wavelength-division multiplexing (WDM) or time-division multiplexing (TDM) regime. To meet the first requirement, the wavelengths of optical carrier wave are usually chosen either in ~ 1.3 or in 1.5 μm region where two windows of transmission loss are located. Concerning the second requirement, however, there are two major limitations imposed on the transmission bit-rate as well as the transmission distance via an optical fiber network. The first limitation comes from the so-called chromatic dispersion or group-velocity dispersion (GVD) effect that means the optical pulses having different spectral components exhibit different propagation velocities along a fiber transmission system. Because of this effect, an ultra-short optical pulse, which contains multi-spectral-components within a considerable spectral width, will become broader in time-scale during propagation within a long fiber system. For this reason, the temporal spacing between two adjacent optical pulses cannot be less than a certain value for a given fiber length, and the transmission bit-rate is limited. The chromatic dispersion of an optical fiber system is defined as [179]

$$D(\lambda) = \frac{1}{L}\frac{\mathrm{d}\tau}{\mathrm{d}\lambda} = \frac{1}{L}\frac{\mathrm{d}}{\mathrm{d}\lambda}\left[-\frac{L\lambda_s^2}{2\pi c}\left(\frac{\mathrm{d}\beta}{\mathrm{d}\lambda}\right)_{\lambda_s}\right] = -\frac{\lambda_s^2}{2\pi c}\left(\frac{\mathrm{d}^2\beta}{\mathrm{d}\lambda^2}\right)_{\lambda_s}, \tag{49}$$

where τ is the time delay for an optical pulse propagating in a single-mode fiber of length L, β is the propagation constant of the fiber, λ_s is the central wavelength of the optical signal, and c is the speed of light. For most standard single-mode fibers the zero-dispersion wavelength is $\lambda_0 \approx 1.3$ μm at which $D(\lambda_0) \approx 0$; in a signal wavelength region of $\lambda_s \approx 1.5$ μm the chromatic dispersion $D(\lambda_s) \approx (15-18)$ ps/km/nm. The chromatic-dispersion-limited transmission distance over this type of fiber (for a 1-dB penalty) is given by [180]

$$B^2 L \cong 6500\ (\mathrm{Gbit/s})^2\mathrm{km}. \tag{50}$$

Here B is the bit-rate and L is the fiber length. The limit, for example, is ~ 65 km at a bit-rate of 10 Gbit/s.

In addition to the limitation from chromatic dispersion, there is another limitation that is related to the spectral broadening of optical pulses propagating in a fiber system. It is known that an optical fiber is a good third-order nonlinear medium, in which many nonlinear optical effects can easily take place. Among these effects, the light-intensity dependent refractive-index change may produce self-modulation of an intense short light pulse during its propagation in the fiber system. Sequentially, this self-modulation effect leads to a spectral self-broadening of the given light pulse.

Some other nonlinear processes, such as four-wave mixing or stimulated scattering may also produce new spectral components or cause further spectral broadening. This kind of spectral broadening may degrade the quality of signal transmission and particularly impose a limitation on the minimum spectral spacing between two adjacent channels in a fiber communication system adopting WDM regime.

The latest development of optical fiber communication technology in the recent 10 years has shown that the optical phase conjugation (OPC) technique can be successfully employed to overcome the limitations from chromatic dispersion and self-modulation (spectral self-broadening) respectively. In this case a special optical phase-conjugator is placed in the middle of two identical single-mode fiber transmission systems, which generates phase-conjugate waves of the input signal waves with an inverse spectral structure. This special technique adopted for fiber communications is called "midway optical phase conjugation (MOPC)" or "mid-span spectral inversion (MSSI). The principle of this technique is based on the theoretical proposal reported by Yariv et al. in 1979 [181]. In this proposal a midway phase-conjugator is placed between two identical fiber systems and to generate a phase conjugate wave at frequency $\omega_{pc} = (\omega_0 - \Omega)$ with respect to the input signal wave of frequency $\omega_s = (\omega_0 + \Omega)$. It was theoretically proven that in this specific case, the chromatic dispersion and self-modulation influence from the first fiber system on the optical signal could be compensated by that from the second fiber system. In that original paper the midway phase-conjugator was suggested to be working with the method of backward nondegenerate FWM under the following condition: $2\omega_0 = \omega_s + \omega_{pc} = (\omega_0 + \Omega) + (\omega_0 - \Omega)$, where ω_0 was the frequency of two counter-propagating pump beams. In 1992, Inoue reinvestigated this issue theoretically and suggested the use of forward nondegenerate FWM in an optical fiber as a new approach of midway phase-conjugation [182]. To fulfill the phase-matching requirement of FWM, it was also suggested that ω_0, ω_s and ω_{pc} should be chosen working in the spectral region near to zero-dispersion wavelength. The first experimental demonstration of MSSI in a dispersion-shifted fiber section using forward FWM was reported in 1993 by Watanabe et al. [183] and subsequently by Jopson et al. [184].

Fig. 30 shows a schematic of an optical fiber communication system containing two identical signal-mode fiber spans with a midway optical phase-conjugator, as well as the compensation of chromatic dispersion and spectral broadening by MSSI technique. For simplicity, the assumed input light pulse has an original Fourier-transform limited spectrum distribution with the central frequency located at $(\omega_0 - \Omega)$. During its propagation over the first fiber span, the pulse envelope gradually broadens due to GVD dispersion, as shown in Fig. 30(b), while its spectrum becomes distorted and broadened owing to self-modulation, as shown in Fig. 30(c). After a midway phase-conjugator, the phase-conjugate pulse is generated at a new central frequency $(\omega_0 + \Omega)$ with an inverse spectrum distribution related to that of the signal pulse. Assuming the red-end spectral-components of the signal pulse propagate faster in the first fiber span than the blue-end, then after passing through a midway phase-conjugator, the red-end components of the signal pulse are converted into the blue-end components of the phase-conjugated pulse and, therefore, will propagate slower in the second fiber span. For that reason, the

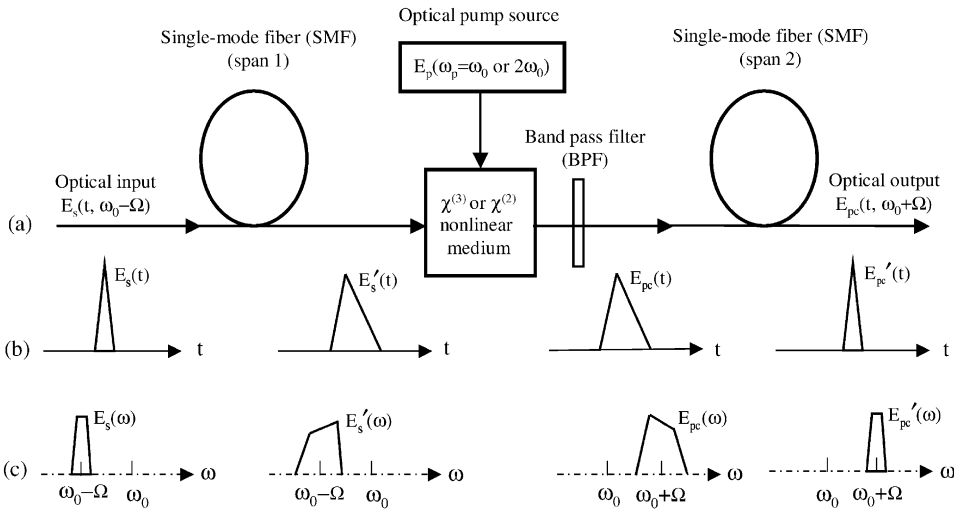

Fig. 30. (a) Schematic diagram showing midway optical phase conjugation (mid-span spectral inversion) between two long spans of single-mode fibers, (b) waveform changes of the input signal pulse and output phase-conjugate pulse, (c) spectrum changes of the input signal pulses and output phase-conjugate pulse.

chromatic dispersion influences from two fiber spans can be cancelled from each other. One may readily realize that the nonlinear self-modulation related spectral broadening influence can also be compensated because of the forward phase-conjugation nature. As we mentioned in Section 3.4, two technical approaches can be used to generate forward PCW with spectral inversion: one is FWM in a third-order ($\chi^{(3)}$) nonlinear medium, and the other is three-wave mixing in a second-order ($\chi^{(2)}$) nonlinear medium. As indicated in Fig. 30(a), the pump frequency should be $\omega_p = \omega_0$ in the former case, whereas $\omega_p = 2\omega_0$ in the latter case. In both cases, the frequency detuning Ω from ω_0 value should be small.

In practice three types of nonlinear media have been employed for MSSI purpose.

7.3.1. Dispersion-shifted fiber (DSF) systems

The most adopted optical fibers for long-distance transmission purpose are conventional single-mode standard fibers with their zero-dispersion wavelength located in $\sim 1.3\,\mu m$ region. However, the most commonly adopted optical wavelengths are chosen in $\sim 1.5\,\mu m$ region because of the low propagation losses and the capability of using erbium-doped fiber amplifier in this spectral region. In order to achieve efficient nondegenerate FWM for MSSI purpose, the so-called dispersion-shifted fiber (DSF) [185–192] can be employed as the nonlinear medium, in which the zero-dispersion wavelength is shifted to the $\sim 1.5\,\mu m$ region. In practice the fiber length used for optical phase-conjugator usually ranges from several km to several tens of km.

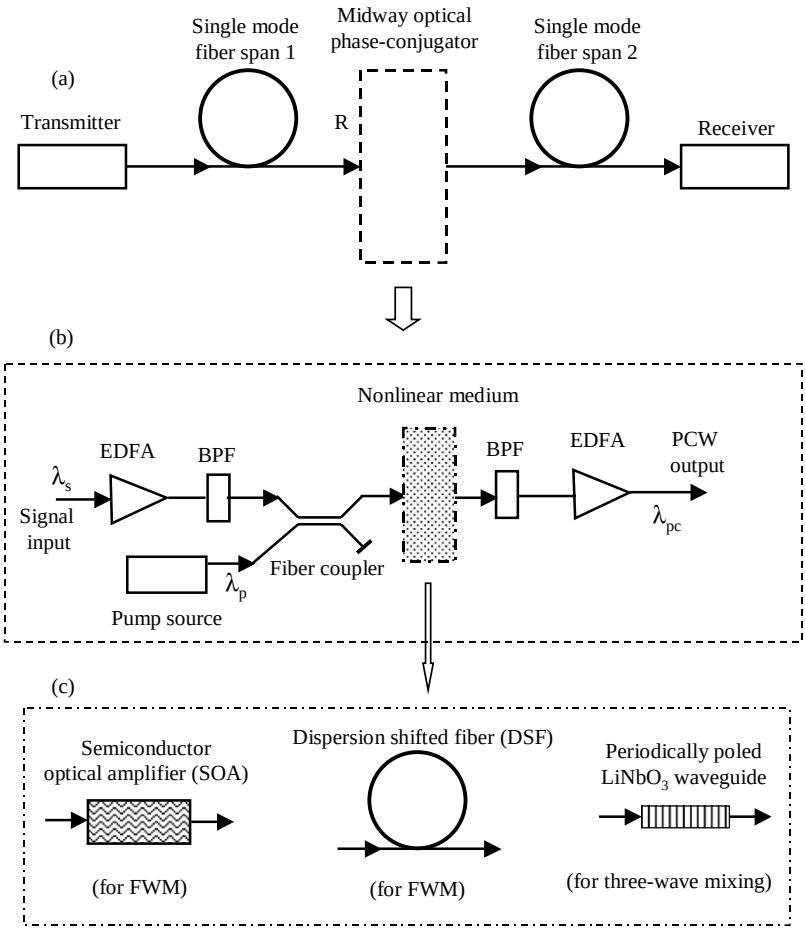

Fig. 31. (a) Midway optical phase conjugation (MOPC) employed in long transmission distance and high bit-rate optical fiber communication systems, (b) basic components of a midway optical phase-conjugator, (c) three types of nonlinear media for MOPC purposes. BPF: band-pass filter; EDFA: erbium-doped fiber amplifier; FWM: four-wave mixing; PCW: phase-conjugate wave.

7.3.2. Semiconductor optical amplifier (SOA) systems

As mentioned in Section 4.3, FWM may efficiently take place in optically pumped lasing media because of their higher effective $\chi^{(3)}$ values. Under those circumstances a higher phase-conjugate output power could be obtained due to the additional simulated amplifying effect. In practice, both the semiconductor optical amplifiers (SOA) [193–198] and semiconductor lasers [199,200] could be employed as midway phase-conjugators for MSSI purpose.

7.3.3. Second-order nonlinear waveguide systems

The advantages of using three-wave mixing in a second-order nonlinear medium to generate forward PCW with spectral inversion are the high efficiency and the

compactness of devices. In practice, a periodically poled $LiNbO_3$ waveguide has been adopted as a midway phase-conjugator for MSSI performance [201,202]. The employed mechanism is the cascaded $\chi^{(2)}$ processes.

Fig. 31 shows schematically the basic components of a generalized midway optical phase-conjugator in a complete modern optical fiber communication system. As shown in Fig. 31(b), after propagating over the first transmission fiber span, the distorted signal pulses pass through an erbium-doped fiber amplifier (EDFA) and a band-pass filter (BPF) then enter the nonlinear medium for wave-mixing. In the mean time, the pump light usually from a semiconductor laser or fiber distributed feedback laser is launched into the same nonlinear medium through a fiber coupler. After completion of four-wave or three-wave mixing, the newly generated phase-conjugate output passes through another BPF and EDFA then enters the second transmission fiber span.

Based on MOPC or MSSI technique, the data-transmission rate and distance through optical fiber links can be significantly increase. For example, at 10 Gbit/s bit-rate the transmission distance through two standard single-mode fiber spans has been increased to 200 km using FWM in a semiconductor optical amplifier (SOA) [203] or 560 km using FWM in a 7.8 km dispersion-shifted fiber (DSF) [204]. At 40 Gbit/s and with a SOA-based phase-conjugator, the fiber transmission distance could be up to 204 km [205]. Furthermore, at an ultra-high bit-rate for 80 Gbit/s, the distance could be up to 106 km using a SOA-based phase-conjugator [206,207].

Finally, it should be noted that the same MOPC principle can also be employed in the future fiber soliton communication systems to improve the optical data transmission rate and quality [208–211].

Acknowledgements

The author wishes to thank Dr. P. N. Prasad, Distinguished Professor and Executive Director of Institute for Lasers, Photonics and Biophonics, State University of New York at Buffalo, for his valuable support in conducting research activity. The author is also indebted to those authors whose works have been quoted in this review article. Finally, T.-C. Lin's assistance is particularly appreciated.

References

[1] A. Yariv, IEEE Journal of Quantum Electronics QE-14 (1978) 650–660.
[2] R.W. Hellwarth, Optical Engineering 21 (1982) 257–262.
[3] R.A. Fisher, (ed.), Optical Phase Conjugation, Academic, New York, 1983.
[4] B.Ya. Zel'dovich, N.F. Pilipetsky, V.V. Shkunov, Principles of Phase Conjugation, Springer-Verlag, Berlin, 1985.
[5] G.S. He, S.H. Liu, Physics of Nonlinear Optics, World Scientific, New Jersey, 2000.
[6] H.J. Eichler, P. Gunter, D.W. Pohl, (ed.), Laser Induced Dynamic Gratings, Springer-Verlag, Berlin, 1986.
[7] M.C. Gower, Progress in Quantum Electronics 9 (1984) 101–147.
[8] V.T. Tikhonchuk, A.A. Zozulya, Progress in Quantum Electronics 15 (1991) 231–293.

[9] R.W. Hellwarth, Journal of the Optical Society of America A67 (1977) 1–3.
[10] D.M. Bloom, G.C. Bjorklund, Applied Physics Letters 31 (1977) 592–594.
[11] B.Ya. Zel'dovich, V.I. Popovichev, V.V. Ragul'skii, F.S. Faizullov, JETP Letters 15 (1972) 109–113.
[12] O.Yu. Nosach, V.I. Popovichev, V.V. Ragul'skii, F.S. Faizullov, JETP Letters 16 (1972) 435–438.
[13] V.G. Koptev, A.M. Lazaruk, I.P. Petrovich, A.S. Rubanov, JETP Letters 28 (1978) 434–436.
[14] G.S. He, Y. Cui, M. Yoshida, P.N. Prasad, Optics Letters 22 (1997) 10–12.
[15] C.V. Heer, N.C. Griffen, Optics Letters 4 (1979) 239–241.
[16] A. Khyzniak, V. Kondilenko, Yu. Kucherov, S. Lesnik, S. Odoulov, M. Soskin, Journal of the Optical Society of America A1 (1984) 169–179.
[17] A. Yariv, Applied Physics Letters 28 (1976) 88–89;
A. Yariv, Journal of the Optical Society of America 66 (1976) 301–306;
A. Yariv, Optics Communications 21 (1977) 49–50.
[18] P.V. Arizonis, F.A. Hopf, W.D. Bamberger, S.F. Jacobs, A. Tomita, K.H. Womack, Applied Physics Letters 31 (1977) 435–437.
[19] N.C. Griffin, C.V. Heer, Applied Physics Letters 33 (1978) 865–866.
[20] N.S. Shiren, Applied Physics Letters 33 (1978) 299–300.
[21] A. Yariv, D.M. Pepper, Optics Letters 1 (1977) 16–18.
[22] R.L. Abrams, R.C. Lind, Optics Letters 2 (1978) 94–96;
R.L. Abrams, R.C. Lind, Erratum 3 (1978) 205.
[23] D.G. Steel, R.C. Lind, J.F. Lam, C.R. Giuliano, Applied Physics Letters 35 (1979) 376–379.
[24] G. Martin, R.W. Hellwarth, Applied Physics Letters 34 (1979) 371–373.
[25] J. Takacs, H.C. Ellin, L. Solymar, Optics Communications 93 (1992) 223–226.
[26] L. Lefort, A. Barthelemy, Optics Letters 21 (1996) 848–850.
[27] F. Devaux, E. Guiot, E. Lantz, Optics Letters 23 (1998) 1597–1599.
[28] G. Eckhardt, R.W. Hellwarth, F.J. McClung, S.E. Schwarz, D. Weiner, E.J. Woodbury, Physical Review Letters 9 (1962) 455–457.
[29] R.Y. Chiao, C.H. Townes, B.P. Stoicheft, Physical Review Letters 12 (1964) 592–595.
[30] D.I. Mash, V.V. Morozov, V.S. Starunov, I.L. Fabelinskii, JETP Letters 2 (1965) 25–27.
[31] G.S. He, P.N. Prasad, Physical Review A 41 (1990) 2687–2697.
[32] D. Liu, G.S. He, Soviet Physics, JETP 88 (1999) 235–245.
[33] G.S. He, P.N. Prasad, Journal of the Optical Society of America B15 (1998) 1078–1085.
[34] G.S. He, N. Cheng, P.N. Prasad, D. Liu, S.H. Liu, Journal of the Optical Society of America B15 (1998) 1086–1095.
[35] S.M. Jensen, R.W. Hellwarth, Applied Physics Letters 32 (1978) 166.
[36] E.E. Bergmann, I.J. Bigio, B.J. Feldman, R.A. Fisher, Optics Letters 3 (1978) 82–84.
[37] M.A. Khan, P.W. Kruse, J.F. Ready, Optics Letters 5 (1980) 261–263.
[38] D. Fekete, J. AuYeung, A. Yariv, Optics Letters 5 (1980) 51–53.
[39] D. Grischkowsky, N.S. Shiren, R.J. Bennett, Applied Physics Letters 33 (1978) 805–807.
[40] D.M. Bloom, P.F. Liao, N.P. Ecnomou, Optics Letters 2 (1978) 58–60.
[41] P.F. Liao, D.M. Bloom, Optics Letters 3 (1978) 4–6.
[42] R.C. Lind, D.G. Steel, M.B. Klein, R.L. Abrams, C.R. Giuliano, R.K. Jain, Applied Physics Letters 34 (1979) 457–459.
[43] A. Tomita, Applied Physics Letters 34 (1979) 463–464.
[44] D. Depatie, D. Haueisen, Optics Letters 5 (1980) 252–254.
[45] R.K. Jain, M.B. Klein, Applied Physics Letters 35 (1979) 454–456.
[46] E.I. Moses, F.Y. Wu, Optics Letters 5 (1980) 64–66.
[47] J. Nilsen, A. Yariv, Optics Communications 39 (1981) 199–204.
[48] Y.L. Guo, M.-Y. Yao, S.-M. Pang, IEEE Journal of Quantum Electronics 20 (1984) 328–331.
[49] H.A. Mac Kenzie, D.J. Hagan, H.A. Al-Attar, IEEE Journal of Quantum Electronics QE-22 (1986) 1328–1340.
[50] M. Ducloy, Applied Physics Letters 46 (1985) 1020–1022.
[51] M.T. De Araujo, S.S. Vianna, G. Grynberg, Optics Communications 80 (1990) 79–83.

[52] N.A. Andreev, V.-I. Bespalov, A.M. Kiselev, A.Z. Matveev, G.A. Pasmanik, A.A. Shilov, JETP Letters 32 (1980) 625–629.
[53] M.D. Skeldon, P. Narum, R.W. Boyd, Optics Letters 12 (1987) 343–345.
[54] A.M. Scott, K.D. Ridlex, IEEE Journal of Quantum Electronics 25 (1989) 438–459.
[55] Y.-S. Kuo, Y.-C. Fong, C. Wu, J.G. McInerney, K. McIver, Optics Communications 97 (1993) 228–232.
[56] M.W. Bowers, R.W. Boyd, IEEE Journal of Quantum Electronics 34 (1998) 634–644.
[57] W.M. Dennis, W. Blau, Optics Communications 57 (1986) 371–375.
[58] A. Costela, J.M. Figuera, F. Florido, Optics Communications 100 (1993) 536–544.
[59] B.R. Reddy, P. Venkateswarlu, Journal of the Optical Society of America B10 (1993) 438–445.
[60] A. Costela, I. Garcia-Moreno, Chemical Physics Letters 249 (1996) 373–380.
[61] S.M. Kuebler, R.G. Denning, Chemical Physics Letters 250 (1996) 120–127.
[62] G.R. Kumar, B.P. Singh, K.K. Sharma, Optics Communications 73 (1989) 81–84.
[63] H. Nakatsuka, D. Masuoka, T. Yamamoto, Optics Communications 80 (1991) 215–218.
[64] E. Mohajerani, E. Whale, G.R. Mitchell, Optics Communications 92 (1992) 403–410.
[65] S. Miyanaga, H. Ohtateme, K. Kawano, H. Fujiwara, Journal of the Optical Society of America B10 (1993) 403–410.
[66] C. O'Neill, V. Blanchet, M.-M.D. Roberge, P. Galarenau, Canadian Journal of Physics 71 (1993) 442–447.
[67] A. Costela, J.M. Figuera, F. Florido, I. Garcia-Moreno, R. Sastre, Optics Communications 119 (1995) 265–274.
[68] R.K. Mohan, C.K. Subramanjan, Optics Communications 144 (1997) 322–330.
[69] R.K. Jain, R.C. Lind, Journal of the Optical Society of America 73 (1983) 647–653.
[70] P. Roussignol, D. Ricard, K.C. Rustagi, C. Flytzanis, Optics Communications 55 (1985) 143–148.
[71] F. Hache, D. Richard, C. Flyzanis, U. Kreibig, Applied Physics A 47 (1988) 347–357.
[72] J.T. Remillard, H. Wang, M.D. Webb, D.G. Steel, IEEE Journal of Quantum Electronics 25 (1989) 408–413.
[73] P. Roussignal, D. Ricard, J. Lukasik, G. Flytzanis, Journal of the Optical Society of America B4 (1987) 5–13.
[74] S.M. Saltiel, B.V. Wonterghem, T.E. Dutton, J.A. Hutchinson, P.M. Rentzepis, IEEE Journal of Quantum Electronics 24 (1988) 2302–2307.
[75] P. Nandakumar, C. Vijavan, Y.V.G.S. Murti, Optics Communications 185 (2000) 457–465.
[76] S.Y. Yuen, P. Becla, Optics Letters 8 (1983) 356–358.
[77] D.G. Steel, S.C. Rand, J. Liu, Journal of the Optical Society of America B4 (1987) 1794–1800.
[78] T. Shimura, S.A. Boothroyd, J. Chrostowski, P. Myslinski, Optics Communications 101 (1993) 124–132.
[79] Y. Zhao, C. Wu, P. Shah, M.K. Kim, L.R. Dawson, Applied Physics Letters 63 (1993) 281–283.
[80] R. Vijava, Y.V.G.S. Murti, G. Sundararajan, C.K. Mathews, P.R. Vasudeva Rao, Optics Communications 94 (1992) 353–356.
[81] A. Costela, I. Carcia-Mareno, J.L. Saiz, Journal of the Optical Society of America B 14 (1997) 615–619k.
[82] A. Costela, I. Garcia-Mareno, J.L. Saiz, Journal of Physical Chemistry B 101 (1997) 4897–4903.
[83] I.C. Khoo, H. Li, Y. Liang, Optics Letters 18 (1993) 1490–1492.
[84] S.-H. Chen, Y. Shen, Journal of the Optical Society of America B 14 (1997) 1750–1753.
[85] A. Miniewicz, S. Bartkiewicz, J. Parka, Optics Communications 149 (1998) 89–95.
[86] I.C. Khoo, Y. Liang, Physical Review E 62 (2000) 6722–6733.
[87] R.A. Fisher, B.J. Feldman, Optics Letters 4 (1979) 140–142.
[88] G.J. Groft, R.P.M. Green, M.J. Damzen, Optics Letters 17 (1992) 920–922.
[89] R.P.M. Green, G.J. Grofts, M.J. Damzen, Optics Communications 102 (1993) 288–292.
[90] A. Brignon, J.-P. Huignard, IEEE Journal of Quantum Electronics 30 (1994) 2203–2210.
[91] R.P.M. Green, G.J. Groft, M.J. Damzen, Optics Letters 19 (1994) 393–395.
[92] A. Brignon, G. Feugnet, J.-P. Huignard, J.-P. Pocholle, Optics Letters 20 (1995) 548–550.
[93] V.V. Krasnikov, V.M. Petnikova, M.S. Pshenishinikov, V.S. Sholomatin, V.V. Shuvalov, Soviet Journal of Quantum Electronics 13 (1983) 983–984.

[94] P.R. Hemmer, D.P. Katz, J. Donoghue, M. Gronin-Golomb, M.S. Shahriar, P. Kumar, Optics Letters 20 (1995) 982–984.
[95] M.Y. Lanzerotti, R.W. Schirmer, A.L. Gaeta, Applied Physics Letters 69 (1996) 1199–1201.
[96] V.S. Sudarshanam, M. Gronin-Golomb, P.R. Hemmer, M.S. Shahriar, Optics Letters 22 (1997) 1141–1143.
[97] D.S. Hsiung, X.-W. Xia, T.T. Grove, M.S. Shahriar, P.P. Hemmer, Optics Communications 154 (1998) 79–82.
[98] M.Y. Lanzerotti, R.W. Schirmer, A.L. Gaeta, G.S. Agarwal, Physical Review A 60 (1999) 4980–4985.
[99] G.C. Cardoso, J.W.R. Tabosa, Optics Communications 185 (2000) 353–358.
[100] T.T. Grove, E. Rousseau, X.-W. Xia, D.S. Hsiung, M.S. Shahriar, P.R. Hemmer, Optics Letters 22 (1997) 1677–1679.
[101] A. Ashkin, G.D. Boyd, J.M. Dziedzic, R.G. Smith, A.A. Ballman, J.J. Levinstein, K. Nassau, Applied Physics Letters 9 (1966) 72–74.
[102] F.S. Chen, J.T. LaMacchia, D.B. Frazer, Applied Physics Letters 13 (1968) 223–225.
[103] P. Yeh, Introduction to Photorefractive Nonlinear Optics, Wiley, New York, 1993.
[104] P. Günter, J.P. Huignard, Photorefractive Materials and Their Applications I &II, Topic in Applied Physics, Vol. 61, Springer-Verlag, Berlin, 1988, 1989.
[105] W.E. Moerner, Scott M. Silence, Chemical Reviews 94 (1994) 127–155.
[106] B. Fischer, S. Sternklar, S. Weiss, IEEE Journal of Quantum Electronics 25 (1989) 550–569.
[107] P. Yeh, IEEE Journal of Quantum Electronics 25 (1989) 484–519.
[108] V. Wang, C.R. Giuliano, Optics Letters 2 (1978) 4–6.
[109] M. Slatkine, I.J. Bigio, B.J. Feldman, R.A. Fisher, Optics Letters 7 (1982) 108–110.
[110] E. Armandilo, D. Proch, Optics Letters 8 (1983) 523–525.
[111] I.V. Tomov, R. Fedosejevs, D.C.D. McKen, Optics Letters 9 (1984) 405–407.
[112] M.T. Duignan, B.J. Feldman, W.T. Whitney, Optics Letters 12 (1987) 111–113.
[113] D.R. Hull, R.A. Lamb, J.R. Digman, Optics Communications 72 (1989) 104–108.
[114] R.P. Johnson, Optics Communications 77 (1990) 231–234.
[115] J.J. Ottusch, D.A. Rockwell, Optics Letters 16 (1991) 369–371.
[116] M.R. Osborne, M.A. O'key, Optics Communications 94 (1992) 346–352.
[117] C.B. Dane, W.A. Neuman, L.A. Hackel, Optics Letters 18 (1992) 1271–1273.
[118] S. Jackel, P. Shalev, R. Lallouz, Optics Communications 101 (1993) 411–415.
[119] R.G. Harrison, V.I. Kovalev, W. Lu, D. Yu, Optics Communications 163 (1999) 208–211.
[120] B.Ya. Zel'dovich, N.A. Mel'nikov, N.F. Pilipetskii, V.V. Ragul'skii, JETP Letters 25 (1977) 36–39.
[121] A.I. Sokolovskaya, G.L. Brekhovskikh, A.D. Kudryavtseva, Soviet Physics, Doklady 22 (1977) 156–158.
[122] A.I. Sokolovskaya, G.L. Brekhovskikh, A.D. Kudryavtseva, Optics Communications 24 (1978) 74–76.
[123] R. Mays, R.J. Lysiak, Optics Communications 31 (1979) 89–92.
[124] I.V. Tomov, R. Fedosejevs, D.C.D. McKen, C. Domier, A.A. Offenberger, Optics Letters 8 (1983) 9–11.
[125] A.I. Sokolovskaya, G.L. Brekhovskikh, A.D. Kudryavtseva, IEEE Journal of Quantum Electronics QE-23 (1987) 1332–1343.
[126] A.D. Kudryavtseva, A.I. Sokolovskaya, J. Gazengel, N. Phu Xuan, G. Rivoire, Optics Communications 26 (1978) 446–448.
[127] J.L. Ferrier, Z. Wu, J. Gazengel, N. Phu Xuan, G. Rivoire, Optics Communications 41 (1982) 135–139.
[128] E.J. Miller, M.S. Malcuit, R.W. Boyd, Optics Letters 15 (1990) 1188–1190.
[129] J. Feinberg, Optics Letters 7 (1982) 486–487.
[130] J.O. White, M. Cronin-Golomb, B. Fischer, A. Yariv, Applied Physics Letters 40 (1982) 450–452.
[131] T.Y. Chang, R.W. Hellwarth, Optics Letters 10 (1985) 408–410.
[132] R.A. Mullen, D.J. Vickers, L. West, D.M. Pepper, Journal of the Optical Society of America B9 (1992) 1726–1734.

[133] Y. Lian, H. Gao, P. Ye, Q. Guan, J. Wang, Applied Physics Letters 63 (1993) 1745–1747.
[134] L. Zhang, Z. Shao, X. Mu, H. Chen, M. Jiang, Optics Communications 123 (1996) 587–591.
[135] R.W. Hellwarth, Journal of the Optical Society of America 68 (1978) 1050–1056.
[136] H. Hsu, S.S. Bor, IEEE Journal of Quantum Electronics 25 (1989) 430–437.
[137] G.G. Kochemasov, V.D. Nikolaev, Soviet Journal of Quantum Electronics 7 (1977) 60–62.
[138] I.M. Bel'dyugin, M.G. Galushkin, E.M. Zemskov, V.I. Mandrosov, Soviet Journal of Quantum Electronics 6 (1976) 1349–1351.
[139] B.Ya. Zel'dovich, V.V. Shkunov, Soviet Journal of Quantum Electronics 7 (1977) 610–615.
[140] N.B. Baranova, B.Ya. Zel'dovich, V.V. Shkunov, Soviet Journal Quantum Electronics 8 (1978) 559–566.
[141] N.B. Baranova, B.Ya. Zel'dovich, Soviet Journal Quantum Electronics 10 (1980) 555–560.
[142] V.I. Bespalov, V.G. Manishin, G.A. Pasmanik, Soviet Physics, JETP 50 (1979) 879–886.
[143] V.G. Sidorovich, V.V. Shkunov, Soviet Physics, Technical Physics 24 (1979) 472–476.
[144] G.S. He, D. Liu, S.H. Liu, Bulletin of the American Physical Society 30 (1985) 1800.
[145] G.S. He, D. Liu, S.H. Liu, Chinese Physics, Lasers 13 (1986) 713–717.
[146] M. Born, E. Wolf, Principles of Optics, 6th Edition, Pergamon, London, 1983, p. 453.
[147] G.S. He, J.D. Bhawalkar, C.F. Zhao, C.K. Park, P.N. Prasad, Optics Letters 20 (1995) 2393–2395.
[148] G.S. He, J.D. Bhawalkar, C.F. Zhao, P.N. Prasad, IEEE Journal of Quantum Electronics 32 (1996) 749–755.
[149] G.S. He, J.D. Bhawalkar, C.F. Zhao, C.K. Park, P.N. Prasad, Applied Physics Letters 68 (1996) 3549–3551.
[150] G.S. He, L. Yuan, Y. Cui, M. Li, P.N. Prasad, Journal of Applied Physics 81 (1997) 2529–2537.
[151] G.S. He, K.S. Kim, L. Yuan, N. Cheng, P.N. Prasad, Applied Physics Letters 71 (1997) 1619–1621.
[152] G.S. He, P.N. Prasad, IEEE Journal of Quantum Electronics 34 (1998) 473–481.
[153] G.S. He, P.P. Markowicz, T.-C. Lin, P.P. Prasad, Nature 415 (2002) 767–770.
[154] G.S. He, J. Dai, T.-C. Lin, N. Cheng, P.P. Markowicz, P.P. Prasad, to be submitted.
[155] M. Sugii, M. Okabe, A. Watanabe, K. Sasaki, IEEE Journal of Quantum Electronics 24 (1988) 2264–2269.
[156] N.A. Kurnit, S.J. Thamas, IEEE Journal of Quantum Electronics 25 (1989) 421–429.
[157] R.J.St. Pierre, D.W. Mordaunt, H. Injeyan, J.G. Berg, R.C. Hillard, M.E. Weber, M.G. Wickham, G.M. Harpole, R. Senn, IEEE Journal of Selected Topics in Quantum Electronics 3 (1997) 53–58.
[158] B. Kralikova, J. Skala, P. Straka, H. Turcicova, Optics Letters 11 (1997) 766–768.
[159] E.J. Friebele, M. Baskansky, J. Reintjes, Electronics Letters 31 (1995) 885–886.
[160] W.H. Richardson, L. Maleki, E. Garmire, IEEE Journal of Quantum Electronics 25 (1989) 382–394.
[161] J.W.R. Tabosa, S.S. Vianna, F.A.M. de Oliveira, Physical Review A 55 (1997) 2968–2972.
[162] L. Lehr, P. Hering, IEEE Journal of Quantum Electronics 33 (1997) 1465–1473.
[163] X.-W. Xia, D. Hsiung, P.S. Bhatia, M.S. Shahriar, T.T. Grove, P.R. Hemmer, Optics Communications 191 (2001) 347–351.
[164] C. Medrano, M. Ingold, P. Günter, Optics Communications 77 (1990) 411–414.
[165] G.W. Ross, R.W. Eason, Optics Letters 18 (1993) 571–573.
[166] M.T. Gruneisen, S.H. Chakmakjian, E.D. Seeberger, D.D. Lockett, C.M. Clayton, Optics Communications 100 (1993) 173–180.
[167] M.W. Wright, J.G. McInerney, C. Wu, Electronics Letters 29 (1993) 1183–1185.
[168] J. Zhang, S.X. Dou, H. Gao, Y. Zhu, P. Ye, Optics Letters 20 (1995) 985–987.
[169] X. Yi, P. Yeh, Optics Communications 107 (1998) 126–130.
[170] W. Wang, A.E. Chiou, G.J. Sonek, M.W. Berns, Journal of the Optical Society of America B14 (1997) 697–707.
[171] G. Yang, A. Siahmakoun, Applied Optics 32 (1993) 1578–1582.
[172] A.-P. Tzannis, P. Beaud, H.-M. Frey, T. Gerber, B. Mischler, P.P. Radi, Applied Optics 36 (1997) 7978–7983.
[173] P.M. Saari, R.K. Kaarli, R.V. Sarapuu, H.R. Sonajalg, IEEE Journal of Quantum Electronics 25 (1989) 339–350.
[174] F. Devaux, G. le Tolguenec, E. Lantz, Optics Communications 147 (1998) 309–312.

[175] Y. Tomita, R. Yahalom, K. Kyuma, A. Yariv, N.S.-K. Kwong, IEEE Journal of Quantum Electronics 25 (1989) 315–338.
[176] S. Tukushima, T. Kurokawa, IEEE Journal of Quantum Electronics 29 (1993) 613–618.
[177] Y. Owechko, IEEE Journal of Quantum Electronics 25 (1989) 619–634.
[178] D.Z. Anderson, J. Feinberg, IEEE Journal of Quantum Electronics 25 (1989) 635–647.
[179] C. Lin, H. Kogelnik, L.G. Cohen, Optics Letters 5 (1980) 476–478.
[180] A.H. Gnauck, R.M. Jopson, R.M. Derosier, IEEE Photonics Technology Letters 5 (1993) 663–666.
[181] A. Yariv, D. Fekete, D.M. Pepper, Optics Letters 4 (1979) 52–54.
[182] K. Inoue, Journal of Lightwave Technology 10 (1992) 1553–1562.
[183] S.S. Watanabe, T. Naito, T. Chikama, IEEE Photonics Technology Letters 5 (1993) 92–95.
[184] R.M. Jopson, A.H. Gnauck, Derosier, Electronics Letters 29 (1993) 576–578.
[185] S. Watanabe, T. Chikama, G. Ishikaula, T. Terahara, H. Kuwahara, IEEE Photonics Technology Letters 5 (1993) 1241–1243.
[186] K. Inoue, T. Hasegawa, K. Oda, H. Toba, Electronics Letters 29 (1993) 1708–1709.
[187] S. Watanabe, T. Chikama, Electronics Letters 30 (1994) 1156–1157.
[188] S. Watanabe, Optics Letters 19 (1994) 1308–1310.
[189] W. Pieper, C. Kurtzke, R. Schnabel, D. Breuer, R. Lundwig, K. Petermann, H.G. Weber, Electronics Letters 30 (1994) 724–725.
[190] A.H. Gnauck, R.M. Jopson, R.M. Derosier, IEEE Photonics Technology Letters 7 (1995) 582–584.
[191] A. Royset, S.Y. Set, I.A. Goncharenko, R.I. Laming, IEEE Photonics Technology Letters 8 (1996) 449–451.
[192] K. Inoue, Optics Letters 22 (1997) 1772–1774.
[193] M.C. Tatham, G. Sherlock, L.D. Westbrook, Electronics Letters 29 (1993) 1851–1852.
[194] R.M. Jopson, R.E. Tench, Electronics Letters 29 (1993) 2216–2217.
[195] S.Y. Set, H. Geiger, R.I. Laming, M.J. Cole, L. Reekie, IEEE Journal of Quantum Electronics 33 (1997) 1694–1698.
[196] J. Inoue, H. Kawaguchi, IEEE Photonics Technology Letters 10 (1998) 349–351.
[197] H.C. Lim, F. Futami, K. Kikuchi, IEEE Photonics Technology Letters 11 (1999) 578–580.
[198] H. Sotobayashi, K. Kitayama, Journal of Lightwave Technology 17 (1999) 2488–2497.
[199] P.P. Iannone, A.H. Gnauck, P.R. Prucnal, IEEE Photonics Technology Letters 6 (1994) 1046–1049.
[200] S. Watanabe, H. Kuwatsuka, S. Takeda, H. Isshikawa, Electronics Letters 33 (1997) 316–317.
[201] I. Brener, B. Mikkelsen, G. Raybon, R. Harel, K. Parameswaran, J.R. Kurz, M.M. Fejer, Electronics Letters 36 (2000) 1788–1790.
[202] D. Kunimatsu, C.Q. Xu, M.D. Pelusi, X. Wang, K. Kikuchi, H. Ito, A. Suzuki, IEEE Photonics Technology Letters 12 (2000) 1621–1623.
[203] M.C. Tatham, X. Gu, L.D. Westbrook, G. Sherlock, D.M. Spirit, Electronics Letters 30 (1994) 1335–1336.
[204] A.H. Gnauck, R.M. Jopson, P.P. Iannone, R.M. Derosier, Electronics Letters 30 (1994) 727–728.
[205] S.Y. Set, S. Yamashita, M. Ibsen, R.I. Laming, D. Nesset, A.E. Kelly, C. Gilbertas, Electronics Letters 34 (1998) 1681–1683.
[206] H.J. Ehrke, E. Patzak, H.G. Weber, T. Merker, IEEE Photonics Technology Letters 11 (1999) 1063–1065.
[207] T. Merker, P. Meissner, U. Feiste, IEEE Journal of Selected Topics in Quantum Electronics 6 (2000) 258–262.
[208] W. Forysiak, N.J. Doran, Electronics Letters 30 (1994) 154–155.
[209] S. Chi, S. Wen, Optics Letters 19 (1994) 1705–1707.
[210] S. Wen, S. Chi, Electronics Letters 30 (1994) 663–664.
[211] T. Hirooka, A. Hasegawa, Electronics Letters 34 (1998) 2056–2057.